Astron. Astrophys. 360, 969–990 (2000)

ASTRONOMY AND ASTROPHYSICS

Irradiation and mass transfer in low-mass compact binaries

H. Ritter[1], **Z.-Y. Zhang**[2,3], **and U. Kolb**[4]

[1] Max-Planck-Institut für Astrophysik, Karl-Schwarzschild-Strasse 1, 85740 Garching, Germany
[2] National Astronomical Observatories, Chinese Academy of Sciences, Beijing 100012, P.R. China
[3] Department of Physics and Astronomy, University of Leicester, Leicester LE1 7RH, UK
[4] Department of Physics and Astronomy, The Open University, Milton Keynes MK7 6AA, UK

Received 20 December 1999 / Accepted 18 May 2000

Abstract. This paper studies the reaction of low-mass stars to anisotropic irradiation and its implications for the long-term evolution of compact binaries (cataclysmic variables and low-mass X-ray binaries).

First, we show by means of simple homology considerations that if the energy outflow through the surface layers of a low-mass main sequence star is blocked over a fraction $s_{\rm eff} < 1$ of its surface (e.g. as a consequence of anisotropic irradiation) it will inflate only modestly, by a factor $\sim (1 - s_{\rm eff})^{-0.1}$. The maximum contribution to mass transfer of the thermal relaxation of the donor star is $s_{\rm eff}$ times what one obtains for isotropic ($s_{\rm eff} = 1$) irradiation. The duration of this irradiation-enhanced mass transfer is of the order of $0.1|\ln(1-s_{\rm eff})|$ times the thermal time scale of the convective envelope. Numerical computations involving full 1D stellar models confirm these results.

Second, we present a simple analytic one-zone model for computing the blocking effect by irradiation which gives results in acceptable quantitative agreement with detailed numerical computations.

Third, we show in a detailed stability analysis that if mass transfer is not strongly enhanced by consequential angular momentum losses, cataclysmic variables are stable against irradiation-induced runaway mass transfer if the mass of the main sequence donor is $M \lesssim 0.7{\rm M}_\odot$. If $M \gtrsim 0.7{\rm M}_\odot$ systems may be unstable, subject to the efficiency of irradiation. Low-mass X-ray binaries, despite providing much higher irradiating fluxes, are even less susceptible to this instability.

If a binary is unstable, mass transfer must evolve through a limit cycle in which phases of irradiation-induced high mass transfer alternate with phases of small (or no) mass transfer. At the peak rate mass transfer proceeds on $s_{\rm eff}$ times the thermal time scale rate of the convective envelope. A necessary condition for the cycles to be maintained is that this time scale has to be much shorter ($\lesssim 0.05$) than the time scale on which mass transfer is driven.

Key words: accretion, accretion disks – stars: binaries: close – stars: evolution – stars: interiors – stars: novae, cataclysmic variables – X-rays: stars

Send offprint requests to: hsr@mpa-garching.mpg.de

1. Introduction

It is only a few years since the realization that irradiation of the donor star of a semi-detached binary by accretion luminosity generated in the vicinity of a compact accretor can have far-reaching consequences for the long-term evolution of such binary systems. Podsiadlowski (1991), treating irradiation in spherical symmetry, first addressed this problem in the context of the evolution of low-mass X-ray binaries (LMXBs). Later, Gontikakis & Hameury (1993), Hameury et al. (1993), and Ritter (1994) pointed out that spherically symmetric irradiation is probably not an adequate approximation for the case in point. Preliminary calculations by Ritter (1994) showed that the reaction of low-mass stars to anisotropic irradiation is qualitatively (and quantitatively) different from that to isotropic irradiation. Subsequently, King et al. (1995, 1996b, 1997), hereafter KFKR95, KFKR96 and KFKR97, Ritter et al. (1995, 1996a,b), Hameury & Ritter (1997), hereafter HR97, and McCormick & Frank (1998), hereafter MF98, have dealt with the case of anisotropic irradiation in various ways and detail. In most of the above-quoted papers reference was made to a paper by the present authors in which a detailed and systematic treatment of the basic properties of anisotropic irradiation of low-mass stars was to be found. The preparation of this material has been much delayed. The main purpose of the present paper is to close this gap in the recent literature, and to provide the base for further research.

For this purpose we shall discuss in Sect. 2 in some detail the basic concepts of computing the mass transfer rate in a semi-detached binary with and without irradiation, and present observational evidence and theoretical arguments in support of the notion of anisotropic irradiation. In Sect. 3 we shall present a simple analytic calculation which shows that the reaction of a low-mass star to anisotropic irradiation is qualitatively and quantitatively different from what one obtains in the isotropic case. We show also that the simple analytic results are fully supported by corresponding calculations of full 1D stellar models (hereafter simply referred to as full stellar models). In Sect. 4 we study the stability of mass transfer in binaries in which the donor star is exposed to irradiation generated by the accreting companion. In Sect. 5 we shall present a more detailed semi-analytic model than the one in Sect. 3 for the reaction of a low-mass star

to anisotropic irradiation in the limit of small fluxes. The implications of the instability against irradiation-induced runaway mass transfer for the long-term evolution of CVs and LMXBs is discussed in Sect. 6. In Sect. 7 we shall present and discuss results of numerical computations of the secular evolution of CVs subject to the irradiation instability. A summary of our main results and our main conclusions are given in the final Sect. 8.

2. Computing the mass transfer rate

In the context of this paper, compact binaries are either cataclysmic variables (CVs) or LMXBs, i.e. systems consisting of a low-mass star (the secondary) with a mass $M_{\rm s} \lesssim 1{\rm M}_\odot$ which fills its critical Roche lobe and transfers matter to a compact companion (the primary), either a white dwarf (in CVs), or a neutron star or a black hole (in LMXBs). The secular evolution of such systems is a consequence of mass loss from the secondary which, in turn, is driven either by the secondary's nuclear evolution or by loss of orbital angular momentum and possibly other mechanisms such as irradiation on which this paper focuses. In the standard picture of the secular evolution see (e.g. King 1988; Kolb & Ritter 1992, hereafter KR92; Ritter 1996) the nature of the compact star is of no importance, i.e. the star is considered as a point mass (of mass M_c). The nature of the compact component is, however, of importance for accretion phenomena occurring in such systems, e.g. dwarf nova and classical nova outbursts in CVs and X-ray bursts in LMXBs, and when illumination of the secondary by radiation generated through accretion is considered, as we shall do in the following. Thus, calculating the standard secular evolution of such a binary reduces to calculating the evolution of a low-mass star under mass loss, where the mass loss rate derives from the boundary conditions imposed by the fact that the star is in a binary. In the simplest case one obtains the mass loss rate $\dot{M}_{\rm s}$ by requiring that the radius of the secondary $R_{\rm s}$ is always exactly equal to its critical Roche radius $R_{\rm R}$. By decomposing the temporal change of $R_{\rm s}$ and $R_{\rm R}$ as (see e.g. Ritter 1988, 1996)

$$\frac{d\ln R_{\rm s}}{dt} = \zeta_S \frac{\dot{M}_{\rm s}}{M_{\rm s}} + \left(\frac{\partial \ln R_{\rm s}}{\partial t}\right)_{\rm th} + \left(\frac{\partial \ln R_{\rm s}}{\partial t}\right)_{\rm nuc} \quad (1)$$

and

$$\begin{aligned}\frac{d\ln R_{\rm R}}{dt} &= \zeta_{\rm R}\frac{\dot{M}_{\rm s}}{M_{\rm s}} + \left(\frac{\partial \ln R_{\rm R}}{\partial t}\right)_{\dot{M}_{\rm s}=0} \\ &= \zeta_{\rm R}\frac{\dot{M}_{\rm s}}{M_{\rm s}} + 2\left(\frac{\partial \ln J}{\partial t}\right)_{\dot{M}_{\rm s}=0} \quad (2)\end{aligned}$$

one obtains

$$\dot{M}_{\rm s} = \frac{M_{\rm s}}{\zeta_S - \zeta_{\rm R}} \times \left[2\left(\frac{\partial \ln J}{\partial t}\right)_{\dot{M}_{\rm s}=0} - \left(\frac{\partial \ln R_{\rm s}}{\partial t}\right)_{\rm th} - \left(\frac{\partial \ln R_{\rm s}}{\partial t}\right)_{\rm nuc}\right] . \quad (3)$$

Here

$$\zeta_S = \left(\frac{\partial \ln R_{\rm s}}{\partial \ln M_{\rm s}}\right)_S \quad (4)$$

is the adiabatic mass radius exponent of the secondary, and

$$\zeta_{\rm R} = \left(\frac{\partial \ln R_{\rm R}}{\partial \ln M_{\rm s}}\right)_* \quad (5)$$

the mass radius exponent of the critical Roche radius, where the subscript * indicates that for evaluating this quantity one has to specify how mass and angular momentum are redistributed in the system. J is the orbital angular momentum, $(\partial \ln R_{\rm s}/\partial t)_{\rm th}$ the rate of change of $R_{\rm s}$ due to thermal relaxation and $(\partial \ln R_{\rm s}/\partial t)_{\rm nuc}$ the one due to nuclear evolution. The virtue of (3) is that it shows immediately how secular evolution works: If the binary is dynamically stable against mass transfer; i.e. if $\zeta_S - \zeta_{\rm R} > 0$, then mass transfer must be driven by some mechanism. This can either be the secondary's expansion due to nuclear evolution or the shrinkage of the orbit due to loss of orbital angular momentum. In the standard evolution of low-mass binaries, mass transfer is usually not driven by thermal relaxation. However, as we shall see below, this is not necessarily true if irradiation of the secondary is taken into account.

Attempts to bring the observed population of millisecond pulsars in line with the death rate of their presumed progenitors, i.e. the LMXBs, have resulted in the speculation that the secular evolution of LMXBs might be drastically different from, and their lifetime much shorter than that of CVs (e.g. Kulkarni and Narayan 1988). A possible reason for this is seen in the fact that the donor in a LMXB is exposed to a high flux of hard X-ray radiation emitted by the accreting compact star. In fact, Podsiadlowski (1991) has shown that irradiating a low-mass main-sequence star ($M \lesssim 0.8{\rm M}_\odot$) spherically symmetrically with a flux $F_{\rm irr} \gtrsim 10^{11} - 10^{12}\,{\rm erg\,cm^{-2}\,s^{-1}}$ results in an expansion of the star on a thermal time scale and in its gradual transformation into a fully radiative star. It is this expansion which can drive mass transfer on a thermal time scale and this was thought to shorten the lifetime of a LMXB. On the formal level the effect of irradiation is taken into account by replacing (1) by

$$\begin{aligned}\frac{d\ln R_{\rm s}}{dt} &= \zeta_S\frac{\dot{M}_{\rm s}}{M_{\rm s}} \\ &+ \left(\frac{\partial \ln R_{\rm s}}{\partial t}\right)_{\rm ml} + \left(\frac{\partial \ln R_{\rm s}}{\partial t}\right)_{\rm nuc} + \left(\frac{\partial \ln R_{\rm s}}{\partial t}\right)_{\rm irr} . \quad (6)\end{aligned}$$

Here, $(\partial \ln R_{\rm s}/dt)_{\rm ml}$ is the thermal relaxation term arising from mass loss alone and $(\partial \ln R_{\rm s}/\partial t)_{\rm irr}$ the thermal relaxation term caused by irradiation (at constant mass). The latter term arises because irradiating the donor star means that its surface boundary conditions are changed and that it tries to adjust to them on a thermal time scale. With (6) instead of (1) we have now for the mass transfer rate

$$\begin{aligned}\dot{M}_{\rm s} &= \frac{M_{\rm s}}{\zeta_S - \zeta_{\rm R}}\Big[2\frac{\partial \ln J}{\partial t} - \left(\frac{\partial \ln R_{\rm s}}{\partial t}\right)_{\rm ml} \\ &- \left(\frac{\partial \ln R_{\rm s}}{\partial t}\right)_{\rm nuc} - \left(\frac{\partial \ln R_{\rm s}}{\partial t}\right)_{\rm irr}\Big] . \quad (7)\end{aligned}$$

From (7) it is clearly seen that if $(\partial \ln R_{\rm s}/\partial t)_{\rm irr} > 0$, irradiation amplifies mass transfer. However, there are limits to what irradiation can do because the time scale and the amplitude of the

effect are limited. The secondary's expansion due to irradiation saturates at the latest when it has become fully radiative, where it is larger by $\delta \ln R_{\rm s}$ than a star of the same mass in thermal equilibrium without irradiation. As we shall show below the time scale τ on which the irradiated star initially expands is of the order of or less than the thermal time scale of the convective envelope $\tau_{\rm ce}$. As a result, we can expect a maximum contribution from irradiation to $\dot{M}_{\rm s}$ at the onset of irradiation (i.e. of mass transfer) which is of the order

$$(-\delta\dot{M}_{\rm s})_{\rm irr} = \frac{M_{\rm s}}{\zeta_S - \zeta_{\rm R}} \left(\frac{\partial \ln R_{\rm s}}{\partial t}\right)_{\rm irr} \lesssim \frac{M_{\rm s}}{\zeta_S - \zeta_{\rm R}} \frac{\delta \ln R_{\rm s}}{\tau} \ . \quad (8)$$

However, with ongoing irradiation not only does $(\partial \ln R_{\rm s}/\partial t)_{\rm irr}$ decrease roughly exponentially on the time scale τ, but other effects also tend to decrease $-\dot{M}_{\rm s}$. With the star's transformation from a mainly convective to a fully radiative structure, ζ_S increases from $-1/3 \lesssim \zeta_S < 0$ to a large positive value. Thus $\zeta_S - \zeta_{\rm R}$ increases, with the result that $-\dot{M}_{\rm s}$ decreases. In addition, even the driving angular momentum loss is affected: for both braking mechanisms discussed in the literature, i.e. magnetic braking (e.g. Verbunt & Zwaan 1981; Mestel & Spruit 1987) and gravitational radiation (e.g. Kraft et al. 1962), $(\partial \ln |\dot{J}|/\partial \ln R_{\rm s}) < 0$. Thus $|\dot{J}|$ decreases if the secondary inflates. Worse, magnetic braking which is thought to be coupled to the presence of a convective envelope might cease altogether once the star has become fully radiative. In this case the system might no longer be able to sustain the mass transfer necessary to keep the secondary in its fully radiative state. As a consequence, it is therefore possible that such systems evolve through a limit cycle in which short phases (of duration τ) with irradiation-enhanced mass transfer alternate with long detached phases during which the oversized secondary shrinks as it approaches thermal equilibrium, again on the thermal time scale, whereas the system contracts on the much longer time scale of angular momentum loss.

A number of theoretical studies along these lines, under the assumption of spherically symmetric irradiation, have been performed (e.g. by Podsiadlowski 1991; Harpaz & Rappaport 1991; Frank et al. 1992; D'Antona & Ergma 1993; Hameury et al. 1993; Vilhu et al. 1994), all more or less confirming the behaviour outlined above, including cyclic evolution (Hameury et al. 1993; Vilhu et al. 1994). It should be stressed once more that the validity of these studies, in which the effect of irradiation is maximized, rests on the validity of the assumption that spherically symmetric irradiation is an adequate approximation. In fact, Gontikakis & Hameury (1993) and Hameury et al. (1993) have examined whether the spherically symmetric approximation is adequate and find that it is not. Worse, when taking into account the anisotropy of the irradiation they find that the long-term evolution differs significantly from the spherically symmetric case. Now, anisotropic irradiation is a rather difficult 3-dimensional problem involving hydrostatic disequilibrium to some extent, and with it circulations which can transport heat from the hot to the cool side of the star. Because of this one might dismiss simple theoretical arguments such as those given by Gontikakis & Hameury (1993) and Hameury et al. (1993). There is, however, a much more compelling argument supporting the case of anisotropic irradiation. This derives from the observations of a number of close but detached binary systems in which a low-mass companion, exposed to an intense radiation field emerging from its hot (degenerate) companion, shows a bright illuminated and an essentially undisturbed cool hemisphere. A compilation of the systems in question is given in Table 1, where we list the object's name, its association with a known planetary nebula, its orbital period (in days), the effective temperature of the irradiating white dwarf, the amplitude (in magnitudes) of the "reflection effect", and relevant references. These systems all show a pronounced "reflection effect"in their light curves which, in turn, is explained by the anisotropic temperature distribution on the irradiated companion. Among them are 7 binary central stars of planetary nebulae. The systems listed in Table 1 demonstrate that a cool star, exposed to strong irradiation from a hot companion, can live without problems with a hot and a cool hemisphere. Moreover equal effective temperature over the whole surface is not established, at least not over atime scale $\sim 10^4$ yr associated with the age of central stars of planetary nebulae, despite the fact that the irradiated star need not even rotate nearly synchronously. Obviously, heat transport from the hot side to the cool side by means of circulations is sufficiently ineffective that the large difference in effective temperatures can be maintained over long times. Thus the case of anisotropic irradiation has to be taken seriously and deserves a more detailed study. This is the objective of this paper.

3. Reaction of a low-mass star upon reducing its effective surface

We start our examination of anisotropic irradiation by recalling one of the main results obtained in the studies of spherically symmetric irradiation (e.g. Podsiadlowski 1991; D'Antona & Ergma 1993), namely that the main effect of irradiating a low-mass main-sequence star is that the star cannot lose energy as effectively (or at all) through the irradiated parts of its surface. If irradiation is spherically symmetric, the star has no choice but to store the blocked energy in gravitational and internal energy with the well-known result that it swells. In the case of anisotropic irradiation, such as one-sided irradiation from an accreting companion, the situation is qualitatively different: in addition to storing the blocked luminosity in internal and gravitational energy, the star can also divert its energy flow to and lose energy from the unirradiated parts of its surface. This is easily possible in the adiabatic convection zone. Because in this zone the energy flow is almost fully decoupled from the mechanical and thermal structure (the flow being proportional to $(\nabla - \nabla_{\rm a})^{3/2}$ with $\nabla - \nabla_{\rm a} \ll 1$ rather than to ∇ (where $\nabla = \partial \ln T/\partial \ln P$ is the actual temperature gradient and $\nabla_{\rm a} = (\partial \ln T/\partial \ln P)_{\rm a}$ the adiabatic temperature gradient, and T and P are respectively the temperature and pressure) the mechanical and thermal structure of the star can still be considered to be spherically symmetric despite the fact that the energy flow might be highly anisotropic. The only thing which

Table 1. Detached close binaries showing a reflection effect

Object	associated planetary nebula	$P_{\rm orb}({\rm d})$	$T_{\rm eff,1}(10^3{\rm K})$	amplitude of reflection effect	Ref.
BE UMa	+	2.2912	105 ± 1	$\Delta m_{\rm pg} = 0.9$	1,2
VW Pyx	K1–2	0.6701	85 ± 6	$\Delta m = 1.5$	3,4
V664 Cas	HFG 1	0.5817		$\Delta B = 1.1$	5,6
V477 Lyr	Abell 46	0.4717	60 ± 10	$\Delta V = 0.6$	7
UU Sge	Abell 63	0.4651	117.5 ± 12.5	$\Delta V = 0.4$	8,9
KV Vel	DS 1	0.3571	77 ± 3	$\Delta V = 0.56$	10,11
TW Crv	—	0.3276		$\Delta V = 0.85$	12
AA Dor	—	0.2615	40 ± 3	$\Delta V = 0.05$	11,13,14
MS Peg	—	0.1737	22.2 ± 0.1	$\Delta V = 0.1$	15
NN Ser	—	0.1301	55 ± 8	$\Delta V = 0.4$	16,17
HW Vir	—	0.1167	33.0 ± 0.8	$\Delta V = 0.2$	11,18,19
MT Ser	Abell 41	0.1132	80 ± 20	$\Delta B = 0.15$	20,21
NY Vir	—	0.1010	33 ± 3	$\Delta V = 0.2$	22

References: 1: Ferguson et al. (1999); 2: Wood et al. (1995); 3: Kohoutek & Schnur (1982); 4: Bond & Grauer (1987); 5: Grauer et al. (1987); 6: Acker & Stenholm (1990); 7: Pollacco & Bell (1994a); 8: Pollacco & Bell (1993); 9: Bell et al. (1994); 10: Landolt & Drilling (1986); 11: Hilditch et al. (1996); 12: Chen et al. (1995); 13: Kilkenny et al. (1979); 14: Kudritzki et al. (1982); 15: Schmidt et al. (1994); 16: Haefner (1989); 17: Catalán et al. (1994); 18: Wlodarczyk & Olszewski (1994); 19: Wood & Saffer (1999); 20: Grauer & Bond (1983); 21: Grauer (1985); 22: Kilkenny et al. (1998).

changes is the surface boundary condition which replaces the Stefan-Boltzmann law in the unirradiated case.

In the following we shall make a simple model for studying the situation described above. In this model we assume that over a fraction $s_{\rm eff}$ of the stellar surface the energy outflow is totally blocked (because of irradiation, or e.g. star spots, see Spruit & Ritter 1983) and that the remaining fraction of the surface $(1 - s_{\rm eff})$ radiates with an effective temperature $T_{\rm eff}$. The surface luminosity of the star L can therefore be written as

$$L(s_{\rm eff}) = 4\pi R^2 (1 - s_{\rm eff}) \sigma T_{\rm eff}^4 \ , \quad 0 \le s_{\rm eff} < 1 \quad , \tag{9}$$

where R is the stellar radius. It is clear that in a more realistic model $s_{\rm eff}$ itself must depend on the irradiating flux $F_{\rm irr}$. In Sect. 4 we shall discuss results of numerical calculations and a model with which we can evaluate $s_{\rm eff}(F_{\rm irr})$. For the moment we note only that $s_{\rm eff} \to 0$ as $F_{\rm irr} \to 0$ and that in the limit of high $F_{\rm irr}$, $s_{\rm eff}$ approaches the surface fraction of the star which sees the irradiation source.

The purpose of this simple modelling is, on the one hand, to provide estimates for the magnitude of and the time scale associated with the thermal relaxation process enforced by anisotropic irradiation, and, on the other hand, to show that the effects of anisotropic irradiation are not only quantitatively but also qualitatively different from those obtained in the spherically symmetric case.

The internal structure of a low-mass star with a deep outer convection zone can be described by the simple analytical model by Kippenhahn & Weigert (1994) for stars on or near the Hayashi line. This model is particularly applicable in our case, since we are only interested in the differential behaviour. Assuming a power law approximation for the frequency independent, i.e. grey photospheric opacity $\kappa_{\rm ph}$ on the unirradiated surface of the form

$$\kappa_{\rm ph} = \text{const.}\ P^a T^b \quad , \tag{10}$$

the Eddington approximation yields the photospheric solution

$$\log T_{\rm eff} = -\frac{a+1}{b} \log P_{\rm ph} + \frac{1}{b} \log M - \frac{2}{b} \log R + \text{const.}, \tag{11}$$

where $P_{\rm ph} = P(\tau = 2/3)$ is the photospheric pressure at an optical depth $\tau = 2/3$. The interior solution can be approximated by a polytrope with index $n = 3/2$ and yields

$$\log T = \frac{2}{5}\ \log P + \frac{2}{5}\left[\frac{3}{2}\ \log R - \frac{1}{2}\ \log M + \text{const.}\right]. \tag{12}$$

Taking (12) at the photospheric point $(P = P_{\rm ph},\ T = T_{\rm eff})$, i.e. equating (11) and (12), together with (9) and (10) yields the luminosity L lost by the star with radius R over the surface area $4\pi R^2(1 - s_{\rm eff})$:

$$L(s_{\rm eff}) = L_0 (1 - s_{\rm eff}) \left(\frac{R}{R_0}\right)^{(22a+4b+6)/(5a+2b+5)} \quad . \tag{13}$$

Here L_0 and R_0 are respectively the luminosity and the radius of the unirradiated star in thermal equilibrium. In general, the irradiated star will not be in thermal equilibrium, i.e. $L(R, s_{\rm eff})$ does not equal the nuclear luminosity $L_{\rm nuc}$. For the disturbed star, the latter can be estimated by using homology relations. If we write the rate of nuclear energy generation $\varepsilon_{\rm nuc}$ in the form appropriate for hydrogen burning via the pp-chain, i.e.

$$\varepsilon_{\rm nuc} = \text{const.}\ \varrho T^\nu \quad , \tag{14}$$

where ϱ is the density, we obtain (see e.g. Kippenhahn & Weigert 1994)

$$L_{\rm nuc}(R) = L_0 \left(\frac{R}{R_0}\right)^{-(\nu+3)} \quad . \tag{15}$$

From (13) and (15) we obtain the gravitational luminosity

$$L_{\rm g}(R, s_{\rm eff}) = L(R, s_{\rm eff}) - L_{\rm nuc}(R) \quad . \tag{16}$$

$L_{\rm g}(R, s_{\rm eff}) = 0$ defines the thermal equilibrium values of the irradiated star. These can be expressed in terms of the thermal equilibrium values of the unirradiated star as follows:

$$R_{\rm e}(s_{\rm eff}) = R_0(1 - s_{\rm eff})^r$$

with (17)

$$r = -\frac{5a + 2b + 5}{(\nu + 3)(5a + 2b + 5) + 22a + 4b + 6} \quad ,$$

$$L_e(s_{\rm eff}) = L_0(1 - s_{\rm eff})^\ell$$

with (18)

$$\ell = -(\nu + 3)r \quad ,$$

and

$$T_{\rm eff}(s_{\rm eff}) = T_{\rm eff,0}(1 - s_{\rm eff})^t$$

with (19)

$$t = \frac{\ell - 2r - 1}{4} \quad .$$

Since the dominant opacity source in the photosphere of cool stars is H^- bound-free absorption, appropriate values for a and b in (10) are $a \approx 0.5$ and $b \approx 4$–5. Nuclear energy generation in low-mass stars occurs mainly via the pp-I chain and the appropriate value of ν in (14) is $\nu \approx 3$–5. As a result, we find that

$$r \approx -0.1$$

$$\ell \approx 0.75 \quad ,$$

and

$$t \approx -0.003 \quad .$$

This means that the effective temperature on the unirradiated part of the surface hardly changes, reflecting a well-known property of stars on or near the Hayashi line. Furthermore, since $r \approx -0.1$, the response of the stellar radius to anisotropic irradiation ($s_{\rm eff} < 1$) is much weaker than if isotropic irradiation is assumed. Specifically, if $s_{\rm eff} \lesssim 0.5$, as is the case for one-sided irradiation by an accreting companion, the equilibrium radius with irradiation is larger than the one without irradiation by at most $\sim 7\%$. On the other hand, the total luminosity L_e is significantly reduced: because of the rather large value of $\nu + 3 \approx 6$–8 already a slight expansion of the star leads to a marked reduction of its nuclear luminosity.

Clearly, our model is not applicable if $s_{\rm eff} \to 1$. This is because on the formal level $L \to 0$ if $s_{\rm eff} \to 1$ (see Eq. 9) and the values of R and $T_{\rm eff}$ in thermal equilibrium with $r < 0$ and $t < 0$ (Eqs. 17 and 19) diverge. There is also a physical reason why this model does not apply in this case: $s_{\rm eff} = 1$ corresponds to strong, spherically symmetric irradiation where the star in thermal equilibrium is fully radiative (e.g. Podsiadlowski 1991), whereas our model applies only to the extent that the star in question retains a deep outer convective envelope, even when irradiated.

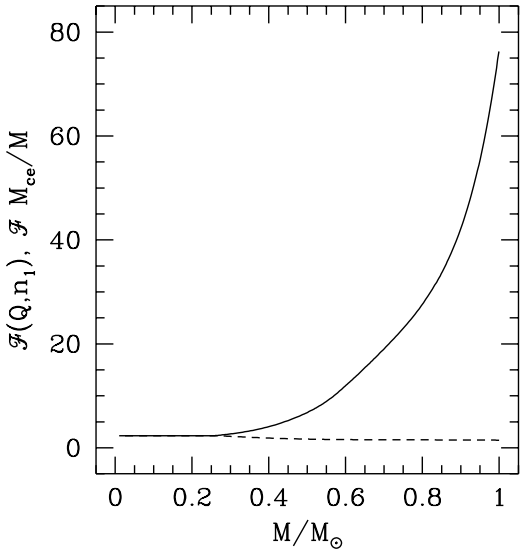

Fig. 1. The function $\mathcal{F}(Q, n_1)$ defined in Eq. (20) (full line) and $\mathcal{F}(Q, n_1)M_{\rm ce}/M$ (dashed line) for age-zero main sequence models in the bipolytrope approximation as a function of mass.

We can now estimate the maximum contribution to mass transfer arising from thermal relaxation due to irradiation and the associated time scale. Thermal relaxation is maximal right at the onset of irradiation. At that time the gravitational luminosity of the star is $L_{\rm g}(R_0, s_{\rm eff}) = -s_{\rm eff}L_0$. Using now the bipolytrope model in the formulation of KR92, we can write for the thermal relaxation term due to irradiation

$$\left(\frac{\partial \ln R}{\partial t}\right)_{\rm irr}\Bigg|_{R=R_0} = -\frac{(L_{\rm g})_{\rm irr}R_0}{GM^2}\,\mathcal{F}(Q, n_1) = \frac{s_{\rm eff}}{\tau_{\rm KH}}\,\mathcal{F}(Q, n_1) = \frac{s_{\rm eff}}{\tau_{\rm ce}} \quad , \tag{20}$$

where $\tau_{\rm KH} = GM^2/R_0L_0$ is the Kelvin-Helmholtz time of the unirradiated star in thermal equilibrium, $\tau_{\rm ce} = \tau_{\rm KH}/\mathcal{F}$ the thermal time scale of the convective envelope, and the quantity $\mathcal{F}(Q, n_1)$ defines a dimensionless number which depends only on the relative size $Q = R_{\rm core}/R_0$ of and on the polytropic index n_1 in the radiative core. An explicit expression for $\mathcal{F}(Q, n_1)$ is given in KFKR96). In particular, for a single polytrope $n = 3/2$, i.e. a fully convective star, where $Q = 0$, one has $\mathcal{F} = 7/3$. Furthermore, we show $\mathcal{F}(Q, n_1)$ as a function of mass for zero age main sequence stars as a full line in Fig. 1. We note that $\mathcal{F}$ scales roughly as the inverse of the relative mass $M_{\rm ce}/M$ of the convective envelope: the dashed line in Fig. 1 shows that $\mathcal{F} \cdot M_{\rm ce}/M \approx$ const. within better than a factor of two. Thus for the purpose of an estimate we can rewrite (20) as

$$\left(\frac{\partial \ln R}{\partial t}\right)_{\rm irr}\Bigg|_{R=R_0} \approx \frac{7}{3}\,\frac{s_{\rm eff}}{\tau_{\rm KH}}\,\left(\frac{M_{\rm ce}}{M}\right)^{-1} \quad , \tag{21}$$

Since the radius in thermal equilibrium with irradiation is larger by

$$\delta \ln R = \ln \frac{R_{\rm e}(s_{\rm eff})}{R_0} = r \ln(1 - s_{\rm eff}) \quad , \tag{22}$$

the time scale for thermal relaxation becomes

$$\tau \approx \delta \ln R \left(\frac{\partial \ln R}{\partial t} \right)^{-1}_{\rm irr} = r \frac{\ln(1 - s_{\rm eff})}{s_{\rm eff}} \tau_{\rm ce}$$
$$\gtrsim r \frac{\ln(1 - s_{\rm eff})}{s_{\rm eff}} \frac{7}{3} \tau_{\rm KH} \frac{M_{\rm ce}}{M} \quad . \tag{23}$$

As can be seen from (21) the maximal rate of expansion is proportional to $s_{\rm eff}$. Interestingly, the time over which the new thermal equilibrium is established is much shorter than if $s_{\rm eff} = 1$, unless $1 - s_{\rm eff}$ is a small number and our model does not apply anyway.

Either (21) or (23) are to be inserted in (8) to get an estimate for the contribution of irradiation to mass transfer. Using (21) in (8) yields the peak contribution and (23) in (8) a time average.

In order to check the validity of our simple analytical model we have also performed numerical computations of full stellar models using the modified Stefan-Boltzmann law (9) as one of the outer boundary conditions and with $s_{\rm eff}$ as a free parameter. For our computations we have used a modified version of Mazzitelli's (1989) stellar evolution code which is described in more detail in KR92, and have assumed a standard Pop. I chemical composition with (in the usual notation) $X = 0.70$ and $Z = 0.02$.

One of the basic predictions of our simple model is that (see Eq. 17) $\log(R_{\rm e}(s_{\rm eff})/R_0)$ scales linearly with $\log(1 - s_{\rm eff})$ and that the slope $|r|$ is small. This is nicely confirmed by the behaviour of full stellar models shown in Fig. 2. As can be seen, the prediction is valid, at least qualitatively, over more than two orders of magnitude of $(1 - s_{\rm eff})$. Furthermore the slope in Fig. 2 is indeed small, confirming that $|r|$ is a small number. That the slope is different for stars of different mass is due to the fact that the effective values of the parameters a, b and ν change with stellar mass.

In Fig. 3 we show in a mass radius diagram the thermal equilibrium radius $R_{\rm e}$ as a function of mass for three different values of $s_{\rm eff}$, i.e. for the standard main sequence ($s_{\rm eff} = 0$), and for $s_{\rm eff} = 0.5$ and $s_{\rm eff} = 0.9$. As can be seen, the mass radius relations for $s_{\rm eff} = 0.5$ and $s_{\rm eff} = 0.9$ are shifted by a small amount to larger radii and run roughly "parallel"to the standard main sequence ($s_{\rm eff} = 0$), as is predicted by our simple model.

Finally, in Fig. 4 we show as an example the thermal relaxation with time of an $0.4 M_\odot$ star with $s_{\rm eff} = 0.5$. If time is measured in units of $(\partial t / \partial \ln R)|_{R=R_0}$, as is done in Fig. 4, it is seen that the relaxation process is characterized by this time scale and that new thermal equilibrium is reached after only 0.2–0.3 of these time units. Again this confirms our analytical result (cf. Eq. 23), according to which the relaxation process lasts a few $r \ln(1 - s_{\rm eff})$ in these units. It is also seen that the effective temperature on the unirradiated part of the star rises only very little, as predicted, but that the relative mass of the

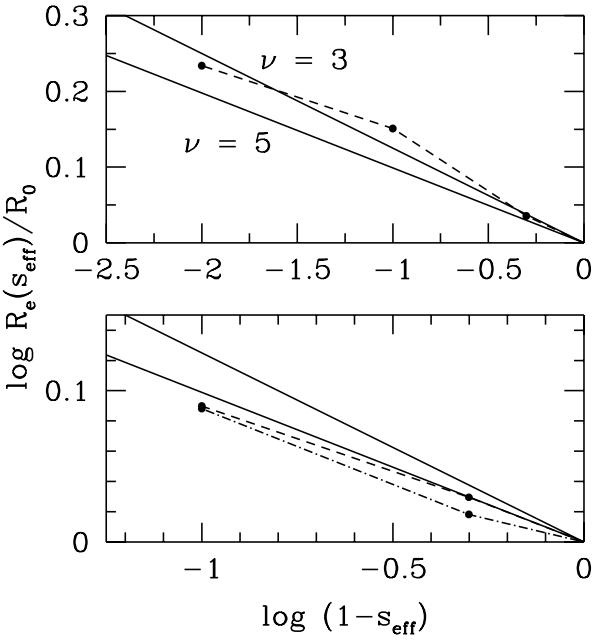

Fig. 2. Radius $R_{\rm e}(s_{\rm eff})$ of homogeneous stellar models in thermal equilibrium as a function of the fraction $s_{\rm eff}$ of the stellar surface over which energy loss is assumed to be blocked. The full lines in both panels show the prediction of the homology model (Eq. 17) with the parameters $a = 0.5$, $b = 4$, and ν as indicated. The dashed line in the upper panel is for full stellar models with a mass of $0.4 M_\odot$, the dashed and dotted lines in the lower panel for full stellar models with a mass of respectively $0.2 M_\odot$ and $0.8 M_\odot$.

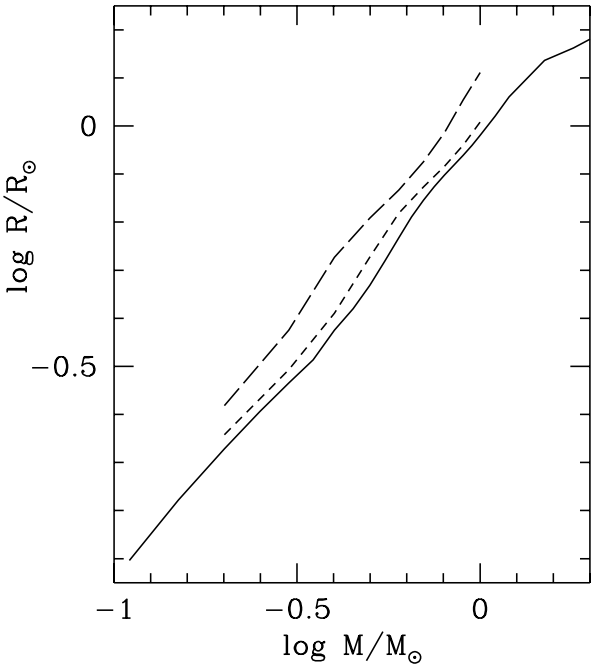

Fig. 3. Mass radius diagram of full stellar models in thermal equilibrium forr three different values of the fraction $s_{\rm eff}$ of the stellar surface over which energy loss is assumed to be blocked. Full line: $s_{\rm eff} = 0$ (normal main sequence); short dashed line: $s_{\rm eff} = 0.5$, and long dashed line: $s_{\rm eff} = 0.9$.

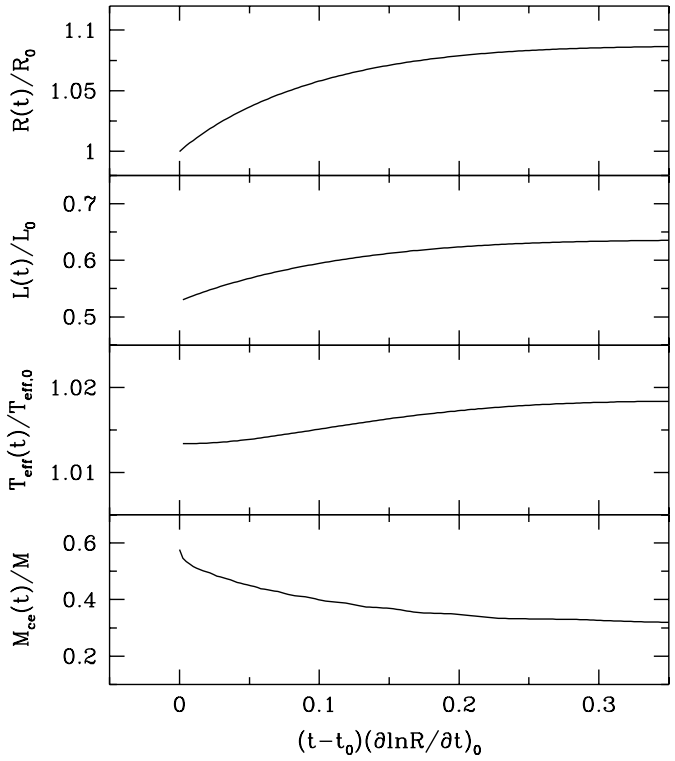

Fig. 4. Thermal relaxation of a $0.4\mathrm{M}_\odot$ main sequence star after blocking the energy loss over a fraction $s_{\rm eff} = 0.5$ of its surface at time $t = t_0$. Top frame: radius R, second frame: luminosity L, third frame: effective temperature $T_{\rm eff}$ of the radiating part, and bottom frame: the relative mass $M_{\rm ce}/M$ of the convective envelope as a function of time. Time is measured in units of the time scale on which the radius grows at $t = t_0$. R_0, L_0, and $T_{\rm eff,0}$ are respectively the values of R, L and $T_{\rm eff}$ immediately before the onset of the blocking of energy outflow.

convective envelope is reduced significantly from ~ 0.6 at the beginning to ~ 0.33 in the new thermal equilibrium.

4. Stability against irradiation-induced mass transfer

Let us now examine the situation in which a low-mass star transfers mass to a compact companion (of mass $M_{\rm c}$ and radius $R_{\rm c}$) and, in turn, is irradiated (directly or indirectly) by the accretion light source. Because irradiation can enhance mass transfer and more irradiation can give rise to even higher mass transfer, we must examine under which conditions such a situation is stable against irradiation-induced runaway mass transfer.

4.1. Arbitrary irradiation geometry

In this subsection we wish to keep the discussion as general as possible. Therefore, we do not specify the irradiation geometry. Specific models which do just that will be presented in Sect. (4.2).

The component normal to the stellar surface of the irradiating flux generated by accretion can be written as

$$F_{\rm irr}(\vartheta,\varphi) = \frac{\eta}{4\pi}\,\frac{GM_{\rm c}(-\dot M_{\rm s})}{R_{\rm c}\,a^2}\,h(\vartheta,\varphi) \quad . \tag{24}$$

Here $-\dot M_{\rm s}$ is the mass transfer rate, a the orbital separation, $h(\vartheta,\varphi)$ a dimensionless function of the position on the secondary's surface (characterized by polar coordinates (ϑ,φ)) which describes the irradiation geometry, and $\eta < 1$ a dimensionless efficiency factor. $\eta = 1$ only if the accretion luminosity is radiated isotropically from the compact star and if all the energy which is radiated into the solid angle subtended by the donor as seen from the accretor is absorbed below the photosphere. In a real situation η will be considerably less than unity for several reasons. The most important of these are: 1) the accretion luminosity will, in general, not be emitted isotropically, e.g. if accretion occurs via a disk which radiates predominantly perpendicular to the orbital plane and casts a shadow onto the donor, or if the accretor is strongly magnetized and accretes mainly near the magnetic poles, as e.g. in AM Her systems. 2) energy emitted in certain spectral ranges, as e.g. EUV radiation and soft X-rays, is unlikely to reach the photosphere of the donor (in the case of EUV and soft X-ray radiation because of the high column density of neutral hydrogen). 3) part of the incident flux will be scattered away before penetrating into the photosphere. 4) not all of the transferred mass needs to be accreted by the compact star. Part of it may leave the system before releasing much potential energy, e.g. via a wind from the outer regions of the accretion disk.

From this it is clear that computing a reliable value for η is a formidable if not nearly impossible task. Therefore, we treat η as a free parameter and our goal must be to arrive at conclusions which are as independent of η as possible.

For deriving the criterion for adiabatic stability against irradiation-induced mass transfer we follow Ritter (1988) (see also Ritter 1996). The only difference is that we use now Eq. (6) instead of (1) (the latter corresponding to Eq. (12) in Ritter's (1988) paper). Accordingly the criterion for adiabatic stability becomes

$$\begin{aligned}\zeta_S - \zeta_{\rm R} > \zeta_{\rm irr} &= -M_{\rm s}\,\frac{\partial}{\partial \dot M_{\rm s}}\left(\frac{\partial \ln R_{\rm s}}{\partial t}\right)\\ &= -M_{\rm s}\,\frac{\partial}{\partial L}\left(\frac{\partial \ln R_{\rm s}}{\partial t}\right)\frac{dL}{d\dot M_{\rm s}} \quad .\end{aligned} \tag{25}$$

The dimensionless number $\zeta_{\rm irr}$ which is defined by (25) measures how sensitively the stellar radius changes in response to irradiation produced by mass transfer. Ignoring the influence of irradiation, i.e. setting $dL/d\dot M_{\rm s} = 0$, gives $\zeta_{\rm irr} = 0$ and (25) reduces to the usual criterion for adiabatic stability.

We compute the derivative $(\partial^2 \ln R_{\rm s}/\partial t \partial L)$ in (25) in the framework of the bipolytrope model (e.g. KR92) from which we obtain (cf Eq. 20)

$$\frac{\partial}{\partial L}\left(\frac{\partial \ln R_{\rm s}}{\partial t}\right) = -\frac{R_{\rm s}}{GM_{\rm s}^2}\,\mathcal{F}(Q,n_1) \quad . \tag{26}$$

For calculating $dL/d\dot M_{\rm s}$ we shall make use of what we shall refer to as the weak irradiation assumption. Making this assumption is tantamount to assuming that at any point (ϑ,φ) lateral heat transport is negligible compared to radial transport. Lateral heat transport occurs in the form of radiative diffusion and advection because of non-vanishing lateral temperature gradients

$\partial T/\partial\vartheta$ and $\partial T/\partial\varphi$, and departures from strict hydrostatic equilibrium. We shall show in the Appendix that the weak irradiation assumption can be justified in those cases we are interested in and that we may safely neglect lateral heat transport. Accordingly, energy conservation requires that at any point (ϑ,φ) the stellar flux, i.e. the energy lost by the star from its interior per unit time and unit surface area is

$$F(\vartheta,\varphi)=\sigma T_{\rm irr}^4(\vartheta,\varphi)-F_{\rm irr}(\vartheta,\varphi) \quad , \tag{27}$$

where $T_{\rm irr}$ is the effective temperature of the surface element in question. With (27) the stellar luminosity, i.e. the energy loss per unit time from the interior becomes

$$L=R_{\rm s}^2\int_0^{2\pi}\int_0^{\pi}F(\vartheta,\varphi)\ \sin\vartheta d\vartheta\, d\varphi \quad . \tag{28}$$

Before working out $dL/d\dot{M}_{\rm s}$ in (25), we shall first examine the reaction of the stellar surface to irradiation in rather general terms. For that it is convenient to introduce the dimensionless irradiating flux

$$x=\frac{F_{\rm irr}}{\sigma T_0^4}=\frac{F_{\rm irr}}{F_0} \tag{29}$$

and the dimensionless stellar flux

$$G=\frac{F}{F_0}=\left(\frac{T_{\rm irr}(x)}{T_0}\right)^4-x=G(x) \quad , \tag{30}$$

where $T_0=T_{\rm eff}(F_{\rm irr}=0)$ is the effective temperature and $F_0=F(F_{\rm irr}=0)=\sigma T_0^4$ the stellar flux in the absence of irradiation. We note that $G(0)=1$ and that we expect $G(\infty)=0$, i.e. that for very high irradiating fluxes energy outflow from the stellar interior is totally blocked. Next we introduce the function

$$g(x)=-\frac{dG}{dx}=-\frac{dF}{dF_{\rm irr}} \quad , \tag{31}$$

which has the following notable properties: First

$$\int_0^{\infty}g(x)dx=G(0)-G(\infty)=1 \tag{32}$$

Second, for positive albedos

$$0<g(x)<1 \quad \forall\, x\geq 0 \quad . \tag{33}$$

Third, if F is a monotonically decreasing function of x (and there is no physical reason why this should not be so), then

$$g'(x)<0 \quad \forall\, x\geq 0 \quad . \tag{34}$$

From (32) and (34) we can immediately prove through integration of $g(x)$ by parts that

$$\mathrm{Max}\,[xg(x)]<1 \quad . \tag{35}$$

The reason why $xg(x)$ attains a maximum can be understood as follows: Rewriting $xg(x)$ in dimensional form (using (29) and (31)) we see that

$$xg(x)=-\frac{F_{\rm irr}}{F_0}\ \frac{dF}{dF_{\rm irr}} \quad . \tag{36}$$

The second factor in (36) describes the incremental blocking of the energy loss from the interior with changing irradiating flux $F_{\rm irr}$. The maximum of $xg(x)$ arises because $-dF/dF_{\rm irr}$ vanishes for large $F_{\rm irr}$. This, in turn, is a consequence of the fact that as long as the star keeps a negative temperature gradient dT/dr in its subphotospheric layer, i.e. the superadiabatic convection zone, irradiation can not block more than the total flux F_0.

As we shall see below, the fact that $xg(x)$ has a maximum is very important for the stability discussion. In fact, we shall see in the next Sect. 5 that for realistic situations the maximum of $xg(x)$ is smaller by about a factor of two than the strict upper limit given by (35).

We can now return to Eq. (28) and compute $dL/d\dot{M}_{\rm s}$. This can be written as

$$\frac{dL}{d\dot{M}_{\rm s}}=-R_{\rm s}^2\int_0^{2\pi}\int_0^{\pi}\frac{dF}{dF_{\rm irr}}\ \frac{dF_{\rm irr}}{d(-\dot{M}_{\rm s})}\ \sin\vartheta d\vartheta d\varphi, \tag{37}$$

where we note that the first factor in the integral is equal to $-g$. With

$$\frac{dF_{\rm irr}}{d(-\dot{M}_{\rm s})}=\frac{F_{\rm irr}(\vartheta,\varphi)}{(-\dot{M}_{\rm s})} \tag{38a}$$

$$=\frac{\eta}{4\pi}\frac{GM_{\rm c}}{R_{\rm c}a^2}\ h(\vartheta,\varphi) \tag{38b}$$

from (24) we have (using (38a))

$$\frac{dL}{d\dot{M}_{\rm s}}=\frac{1}{4\pi}\frac{L_0}{(-\dot{M}_{\rm s})}\left(\frac{R_{\rm s}}{R_0}\right)^2\times \int_0^{2\pi}\int_0^{\pi}x(\vartheta,\varphi)\,g(x(\vartheta,\varphi))\ \sin\vartheta d\vartheta d\varphi\ , \tag{39}$$

where $L_0=4\pi R_0^2\sigma T_0^4$ is the luminosity of the star in thermal equilibrium without irradiation. Combining now Eqs. (25), (26) and (39) we can rewrite the stability criterion as

$$\zeta_S-\zeta_{\rm R}>\zeta_{\rm irr}=\frac{1}{4\pi}\frac{\tau_{M_{\rm s}}}{\tau_{\rm KH}}\ \mathcal{F}(Q,n_1)\left(\frac{R_{\rm s}}{R_0}\right)^3\times \int_0^{2\pi}\int_0^{\pi}x(\vartheta,\varphi)\,g(x(\vartheta,\varphi))\ \sin\vartheta d\vartheta d\varphi \tag{40}$$

or

$$\Lambda\equiv 2(\zeta_S-\zeta_{\rm R})\ \frac{\tau_{\rm KH}}{\tau_{M_{\rm s}}}\ \mathcal{F}^{-1}(Q,n_1)\left(\frac{R_{\rm s}}{R_0}\right)^{-3} > \frac{1}{2\pi}\int_0^{2\pi}\int_0^{\pi}x(\vartheta,\varphi)\,g(x(\vartheta,\varphi))\ \sin\vartheta d\vartheta d\varphi\equiv I \quad , \tag{41}$$

where

$$\tau_{M_{\rm s}}=\frac{M_{\rm s}}{-\dot{M}_{\rm s}} \tag{42}$$

is the mass loss time scale. Although the relations (40) and (41) do not show an explicit dependence on η they nevertheless depend on it via x. However, because of the fact that $xg(x)$ has

a maximum, the integral on the right-hand side of (40) and (41) must have a maximum that is smaller than Max$(xg(x))$. Hence we can state that systems which fulfill the condition

$$\Lambda > \frac{1}{2\pi}\mathrm{Max}\left[\int_0^{2\pi}\int_0^{\pi} x(\vartheta,\varphi)g(x(\vartheta,\varphi))\sin\vartheta d\vartheta d\varphi\right] \ , \quad (43)$$

which *is* independent of η, are definitely stable against irradiation-induced runaway mass transfer.

The reason for rewriting the stability criterion (40) in the form of (41) or (43) is that in the latter conditions Λ does not depend on irradiation but only on the internal structure of the donor star (via ζ_S, $\tau_{\rm KH}$, $\mathcal{F}(Q,n_1)$, R_0) and on the secular evolution model (via $\tau_{M_{\rm s}}$, $\zeta_{\rm R}$ and $R_{\rm s}$). On the other hand, all the information about the irradiation model is contained in the expression on the right-hand side.

For discussing the stability of mass transfer in the limit of very small irradiating fluxes, i.e. $x \to 0$, we must use (38b) instead of (38a) in (39). This results in the following stability criterion:

$$\zeta_S - \zeta_{\rm R} > \zeta_{\rm irr} = \frac{\eta}{4\pi}\frac{M_{\rm c}}{M_{\rm s}}\frac{R_{\rm s}}{R_{\rm c}}\left(\frac{R_{\rm s}}{a}\right)^2 \mathcal{F}(Q,n_1)\times$$
$$\int_0^{2\pi}\int_0^{\pi} g(x(\vartheta,\varphi))\,h(\vartheta,\varphi)\,\sin\vartheta d\vartheta d\varphi \quad . \quad (44)$$

or

$$\Gamma \equiv 2(\zeta_S-\zeta_{\rm R})\,\frac{M_{\rm s}}{M_{\rm c}}\frac{R_{\rm c}}{R_{\rm s}}\left(\frac{a}{R_{\rm s}}\right)^2\mathcal{F}^{-1}(Q,n_1)$$
$$> \frac{\eta}{2\pi}\int_0^{2\pi}\int_0^{\pi} g(x(\vartheta,\varphi))\,h(\vartheta,\varphi)\,\sin\vartheta d\vartheta d\varphi \quad . \quad (45)$$

Because of (34) we arrive at a necessary and sufficient condition for stability

$$\Gamma > \frac{\eta}{2\pi}\,g(0)\int_0^{2\pi}\int_0^{\pi} h(\vartheta,\varphi)\,\sin\vartheta d\vartheta d\varphi \quad . \quad (46)$$

As above, we have separated in the conditions (45) and (46) factors which do not depend on irradiation (collected in Γ) from those which do (on the right-hand side). Like Λ, Γ depends only on the internal structure of the donor star and the secular evolution model. In essence, Eqs. (45) and (46) are conditions on the value of η in the sense that for a given irradiation model, i.e. given $h(\vartheta,\varphi)$ and $g(x)$, η must not exceed a certain value if mass transfer is to be stable.

Furthermore, Eqs. (45) and (46) show in particular that because $g(x)$ is maximal for $x = 0$ (see Eq. 34), i.e. for $F_{\rm irr} = 0$, systems with an unirradiated donor star are the most susceptible to irradiation. In other words, if a system is stable at the turn-on of mass transfer it will remain so later, unless secular effects diminish the value of Γ.

4.2. Specific irradiation models

In the following we describe two specific irradiation models, a rather simple one, hereafter referred to as the constant flux or constant temperature model, and a more realistic one, hereafter referred to as the point source model.

4.2.1. The constant flux model

In this model we assume a fraction $s(\approx 0.5)$ of the stellar surface to be irradiated by a constant average normal flux

$$\langle F_{\rm irr}\rangle = \frac{\eta}{8\pi}\frac{GM_{\rm c}(-\dot{M}_{\rm s})}{R_{\rm c}\,a^2} \quad . \quad (47)$$

Note that the parameter s, introduced above, and $s_{\rm eff}$ which we have introduced in Sect. 3 are not the same quantity. However, s and $s_{\rm eff}$ are related and the corresponding relation will be given below.

Comparison of (47) with (24) shows that we may write $h(\vartheta,\varphi)$ as follows:

$$h(\vartheta,\varphi) = \begin{cases} \frac{1}{2}\ , & 0 \le \vartheta < \vartheta_{\max}\ , \quad 0 \le \varphi \le 2\pi \\ 0\ , & \vartheta_{\max} \le \vartheta \le \pi\ , \quad 0 \le \varphi \le 2\pi \end{cases} \ , \quad (48)$$

where now ϑ is the colatitude with respect to the substellar point and φ the azimuth around the axis joining the two stars. If the star is assumed to be spherical, the colatitude $\vartheta_{\max}$ of the "terminator"of the irradiated part of the surface and s are related via

$$s = \frac{1}{2}\,(1-\cos\vartheta_{\max}) \quad . \quad (49)$$

With (48) and (49), and $\langle x\rangle = \langle F_{\rm irr}\rangle/F_0$, the stability conditions (41) and (45) become respectively

$$\Lambda > 2s\langle x\rangle g(\langle x\rangle) \quad (50)$$

and

$$\Gamma > \eta\, s\, g(\langle x\rangle) \quad . \quad (51)$$

These are the results presented earlier in Ritter et al. (1995, 1996a).

Because of (48) not only is the irradiating normal flux constant but also the effective temperature on the irradiated part (hence the name constant temperature model). (48) inserted in (28) yields the luminosity of the star

$$L = 4\pi R_{\rm s}^2\left[s(\sigma T_{\rm irr}^4 - \langle F_{\rm irr}\rangle) + (1-s)\sigma T_0^4\right] \quad . \quad (52)$$

Comparing this modified Stefan-Boltzmann law with (9) yields the relation between s and $s_{\rm eff}$:

$$s_{\rm eff} = s\left[1 - \frac{\sigma T_{\rm irr}^4 - \langle F_{\rm irr}\rangle}{\sigma T_0^4}\right] = s\,[1-G(\langle x\rangle)] \quad . \quad (53)$$

4.2.2. The point source model

In this model, which has already been discussed in some detail by KFKR96, we assume the donor star to be irradiated by a point source at the location of the compact star. For simplicity we assume the secondary to be spherical. The chosen geometry is axisymmetric with respect to the axis joining the two stars. Denoting again by ϑ the colatitude of a point on the surface of the irradiated star with respect to the substellar point (for a sketch of the geometry see Fig. 5), $h(\vartheta,\varphi)$ in (24) becomes

$$h(\vartheta) = \frac{\cos\vartheta - f_{\rm s}}{(1-2f_{\rm s}\cos\vartheta + f_s^2)^{3/2}} \quad , \quad (54)$$

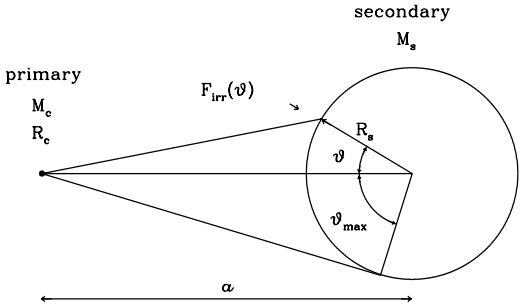

Fig. 5. Sketch of the geometry of the point source model involving a spherical secondary irradiated by a point source at a distance a. Note that $F_{\rm irr}(\vartheta)$ is the irradiating flux normal to the stellar surface.

where

$$f_{\rm s} = \frac{R_{\rm s}}{a} = f_{\rm s}\left(\frac{M_{\rm c}}{M_{\rm s}}\right) \tag{55}$$

is the secondary's radius in units of the orbital separation a. Because the secondary fills its critical Roche volume, $f_{\rm s}$ is a function only of the mass ratio $M_{\rm c}/M_{\rm s}$. The terminator of the irradiated part of the star is at the colatitude

$$\vartheta_{\rm max} = \arccos(f_{\rm s}) \quad . \tag{56}$$

Inserting (54) in (41) or (45), the stability criteria become respectively

$$\Lambda > \int_0^{\vartheta_{\rm max}} x(\vartheta)\, g(x(\vartheta))\, \sin\vartheta d\vartheta = I_{\rm PS} \tag{57}$$

and

$$\Gamma > \eta \int_0^{\vartheta_{\rm max}} g(x(\vartheta))\, h(\vartheta)\, \sin\vartheta d\vartheta \quad . \tag{58}$$

With (54) inserted in (28), the luminosity of the star is

$$L = 4\pi R_{\rm s}^2 \sigma T_0^4 \times \left\{\frac{1}{2}(1+f_{\rm s}) + \frac{1}{2}\int_0^{\vartheta_{\rm max}} G(x(\vartheta))\, \sin\vartheta\, d\vartheta\right\} \quad . \tag{59}$$

Comparing (59) with (9) we find that the effective fraction of the stellar surface over which the energy outflow is blocked is

$$s_{\rm eff} = \frac{1}{2}\left\{1 - f_{\rm s} - \int_0^{\vartheta_{\rm max}} G(x(\vartheta))\, \sin\vartheta\, d\vartheta\right\} \quad . \tag{60}$$

5. The reaction of the subphotospheric layers to irradiation

From the stability analysis we have carried out in the previous section it is clear that we need to know more about the functions $G(x)$ or $g(x)$ (cf. Eqs. 30 and 31) if we wish to use the stability criteria in a quantitative way. So far we know only the properties detailed in Eqs. (32)–(35). These, however, are insufficient for our purposes. Therefore, in this section we shall first use a simple model to derive $g(x)$ explicitly and thereafter discuss results of numerical calculations. As in Sect. 4 we shall adopt the weak irradiation assumption. In this approximation the relation between the stellar flux F and the irradiating flux $F_{\rm irr}$ is a purely local property.

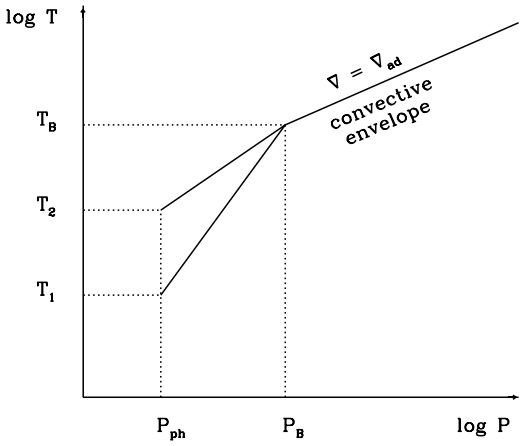

Fig. 6. Sketch of the temperature pressure stratification adopted in the framework of the one-zone model described in Sect. 5.1.

5.1. A one-zone model for the superadiabatic layer

For determining $F(F_{\rm irr})$ we need now a more detailed model of the stellar structure than the one we have assumed in Sect. 3. Whereas in Sect. 3 we have assumed with Kippenhahn & Weigert (1994) that the convective envelope remains adiabatic up to the photosphere, we shall now relax this assumption and take into account the existence of a thin superadiabatic convection zone below the photosphere where convection itself is ineffective as a means of energy transport and energy flows mainly via radiative diffusion. Sufficiently deep in the star, where convection is effective, i.e. adiabatic, the thermal and mechanical structure of the envelope remain spherically symmetric to a very good approximation even in the presence of anisotropic irradiation at the surface (cf. our discussion in Sect. 2). It is only the very thin superadiabatic layer (with a mass of typically $10^{-10}{\rm M}_\odot$), where energy is mainly transported via radiation, which is strongly affected by irradiation. It is this property which allows us to make the weak irradiation assumption, i.e. to treat the effects of irradiation in a local approximation and with the following simple model.

For this we adopt for the moment the temperature-pressure stratification shown in Fig. 6. This means that we replace the "true" structure by one in which we assume convection to be adiabatic out to a point where the pressure is $P = P_{\rm B}$ and the temperature $T = T_{\rm B}$ (where the subscript B stands for the base of the superadiabatic zone). The superadiabatic convection zone extends from the point $(P_{\rm B}, T_{\rm B})$ up to the photosphere where $P = P_{\rm ph}$ and $T = T_{\rm eff}$. Because in this zone convection is ineffective, we make the simplifying assumption that energy transport is via radiation only, i.e. that $\nabla = \nabla_{\rm rad}$, where $\nabla_{\rm rad}$ is the radiative temperature gradient. Because on an irradiated part $T_{\rm eff} = T_{\rm irr} > T_0$, where T_0 is the effective temperature in the absence of irradiation, but $T_{\rm B}$ is assumed to be the same irrespective of irradiation, we see that irradiation, by raising the effective temperature, reduces the temperature gradient ∇ and thus the radiative energy loss through these layers. The superadiabatic layer works like a valve which is open if there is no external irradiation and which closes in progression with the

irradiating flux. As sketched in Fig. 6 we assume for simplicity that $P_{\rm ph}$ does not depend on $F_{\rm irr}$, i.e. on $T_{\rm eff}$.

We can now to derive $T_{\rm irr}(F_{\rm irr})$ by making a simple one-zone model for the superadiabatic layer. For this we shall furthermore assume that the optical depth through this layer is large enough for the diffusion approximation to hold. Then the radiative flux is given by

$$F_{\rm rad} = F = -\frac{ac}{3\kappa\varrho}\frac{dT^4}{dr} \quad , \tag{61}$$

where ϱ is the density, κ the opacity and the other symbols have their usual meaning.

Now we consider the transported flux in two different superadiabatic layers (using subscripts 1 and 2) on an arbitrary isobar at some level $P_{\rm ph} < P_1 = P_2 < P_{\rm B}$. The radiative fluxes are then

$$F_i = -\frac{ac}{3\kappa_i\varrho_i}\left(\frac{dT^4}{dr}\right)_{\rm i} , \quad i = 1,2 \quad . \tag{62}$$

Therefore

$$\frac{\kappa_1\varrho_1}{\kappa_2\varrho_2} = \frac{F_2}{F_1}\,\frac{(dT^4/dr)_1}{(dT^4/dr)_2} \quad . \tag{63}$$

Now we use for the opacity a power-law approximation of the form (10) and the ideal gas equation

$$P = \frac{\mathcal{R}}{\mu}\,\varrho T \quad , \tag{64}$$

where $\mathcal{R}$ is the gas constant and μ the mean molecular weight. Since in the regions of interest the dominant species (H and He) are neutral, we may assume $\mu_1 = \mu_2$. Thus with $P_1 = P_2$ we have

$$\varrho_1 T_1 = \varrho_2 T_2 \quad . \tag{65}$$

Inserting now (10) and (65) into (63) we obtain

$$\frac{F_1}{F_2} = \frac{T_1^{1-b}(dT^4/dr)_1}{T_2^{1-b}(dT^4/dr)_2} = \begin{cases} \frac{(dT^{5-b}/dr)_1}{(dT^{5-b}/dr)_2} \ , & 5-b \neq 0 \\ \\ \frac{(d\ln T/dr)_1}{(d\ln T/dr)_2} \ , & 5-b = 0 \end{cases} . \tag{66}$$

Now we make the one-zone approximation by writing

$$\begin{aligned} \tfrac{dT^n}{dr} &= \tfrac{T^n(P=P_{\rm B}) - T^n(P=P_{\rm ph})}{\Delta r} = \tfrac{T_{\rm B}^n - T_{\rm eff}^n}{\Delta r} \\ \tfrac{d\ln T}{dr} &= \tfrac{\ln T(P=P_{\rm B}) - \ln T(P=P_{\rm ph})}{\Delta r} = \tfrac{\ln T_{\rm B} - \ln T_{\rm eff}}{\Delta r} \quad . \end{aligned} \tag{67}$$

If we now identify layer 1 with the unirradiated one, i.e. set $F_1 = F_0$ and $T_{{\rm eff},1} = T_0$, and layer 2 with an irradiated one, i.e. set $F_2 = F$ and $T_{{\rm eff},2} = T_{\rm irr}$ we obtain by inserting (67) into (66)

$$\frac{F_0}{F} = \frac{1}{G} = \frac{\sigma T_0^4}{\sigma T_{\rm irr}^4 - F_{\rm irr}} = \begin{cases} \frac{T_{\rm B}^{5-b} - T_0^{5-b}}{T_{\rm B}^{5-b} - T_{\rm irr}^{5-b}} \ , & b-5 \neq 0 \\ \\ \frac{\ln T_{\rm B} - \ln T_0}{\ln T_{\rm B} - \ln T_{\rm irr}} \ , & b-5 = 0 \end{cases} , \tag{68}$$

where we have assumed for simplicity $\Delta r_1 = \Delta r_2$. Eq. (68) can be solved for $T_{\rm irr} = T_{\rm irr}(T_0, T_{\rm B}, F_{\rm irr})$, thus providing $G(x, T_{\rm B})$. Thus (68) together with (28) or special cases thereof (Eqs. 52 or 59) can be used as an outer boundary condition for numerical computations.

Let us now briefly consider the consequences of our above assumptions that $P_{{\rm ph},1} = P_{{\rm ph},2}$ and $\Delta r_1 = \Delta r_2$. Because the dominant opacity source is H^- and therefore the opacity increases steeply with temperature, the photospheric pressure on an irradiated, hotter part of the star will be lower than on an unirradiated part (because $P_{\rm ph} \sim g/\kappa$, where g is the surface gravity). Furthermore, the hotter the surface, the further out the photospheric point will be, i.e. $\Delta r_2 > \Delta r_1$ in the above calculation. Because $P_{{\rm ph},2} < P_{{\rm ph},1}$, the temperature gradient ∇_2 below an irradiated part will be higher when setting $P_{{\rm ph},2} = P_{{\rm ph},1}$ rather than using the proper value of $P_{{\rm ph},2}$. Therefore by assuming $P_{{\rm ph},2} = P_{{\rm ph},1}$ we overestimate the radiative flux on the irradiated part. We obtain the same result from using $\Delta r_2 = \Delta r_1$: because in reality $\Delta r_2 > \Delta r_1$, the temperature gradient (67) on an irradiated part is lower than what our estimate with $\Delta r_2 = \Delta r_1$ yields. Therefore, our very simple one-zone model, i.e. Eq. (68) underestimates the blocking effect somewhat. Since, on the one hand, this deficit can easily be compensated for by slightly increasing the value of b, and since, on the other hand, the precise value of b which is appropriate is not exactly determined within our model (we shall later take an average value determined from published opacity tables), we consider (68) a fair approximation of the physical situation described. The really important aspect of our model is, however, that qualitatively it yields the correct behaviour of a stellar surface exposed to external irradiation, and that it is still simple enough to allow insight in the situation described.

We can also compute $g = -dG/dx$. Differentiation of (68) yields

$$g \quad = \begin{cases} \frac{nT_0^4 T_{\rm irr}^{n-1}}{nT_0^4 T_{\rm irr}^{n-1} + 4T_{\rm irr}^3 (T_{\rm B}^n - T_0^n)} \ , & n = 5-b \neq 0 \\ \\ \frac{T_0^4}{T_0^4 + 4T_{\rm irr}^4 \ln(T_{\rm B}/T_0)} \ , & n = 5-b = 0 \end{cases} , \tag{69}$$

if $T_{\rm irr} < T_{\rm B}$. For consistency with Eq. (32) we require $g = 0$ if $T_{\rm irr} > T_{\rm B}$.

As can be seen from Eqs. (68) and (69) the functions G and g depend only on two parameters characterizing the unirradiated star, namely on T_0 and $T_{\rm B}$, and on the opacity law via b. While T_0 is a well-defined quantity, $T_{\rm B}$ is not because in real stars the run of temperature T with pressure P is not as simple as the one assumed in our simple model (and sketched in Fig. 6). In particular, the transition from convective to radiative energy transport is smooth and does not occur at one particular point as we have assumed in our model. Since $T_{\rm B}$ stands for the temperature at which this transition occurs, we determine $T_{\rm B}$ by requiring that in a full stellar model the ratio $F_{\rm conv}/F_{\rm rad}$ of convective flux $F_{\rm conv}$ to radiative flux $F_{\rm rad}$ reaches a prescribed value, say $F_{\rm conv}/F_{\rm rad} = k$. This is equivalent to the condition $\nabla_{\rm rad} = (k+1)\nabla$. Of course the choice of k is somewhat arbitrary but a value $k \approx 1$ seems a natural choice. Our simple model is an acceptable description of the real situation only if for a given model $T_{\rm B}(k)$ is sufficiently insensitive to k. In order

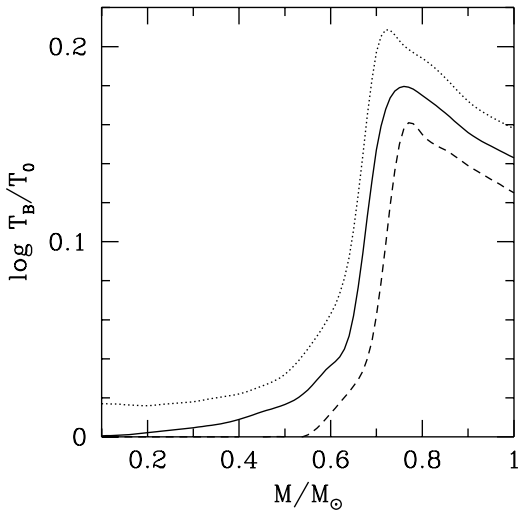

Fig. 7. Temperature $T_{\rm B}$ of the point in the superadiabatic convection zone of a main sequence star $F_{\rm conv}/F_{\rm rad} = k$, or $\nabla_{\rm rad} = (k+1)\nabla$ for $k = 0.5$ (dashed line), $k = 1$ (full line), and $k = 2$ (dotted line) as a function of stellar mass. $T_{\rm B}$ is measured in units of T_0, the effective temperature of the unirradiated star.

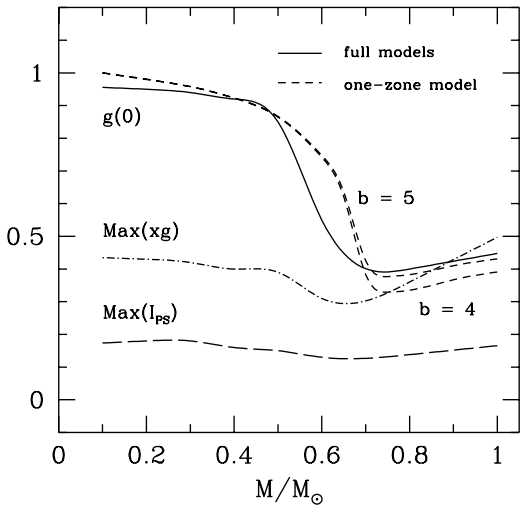

Fig. 8. The values of $g(x{=}0)$ (see Eq. 31) for main sequence stars as a function of stellar mass. Results from full stellar models from HR97 are shown as a full line, results obtained from the one-zone model (Eq. 69) as short-dashed lines. For comparison we show also the run of $\mathrm{Max}[xg(x)]$ (dash-dotted line) and $\mathrm{Max}(I_{\rm PS})$ (long dashed line) derived from the results of HR97).

to demonstrate that this is indeed the case we plot in Fig. 7 the run of $T_{\rm B}$ as a function of the stellar mass of zero-age main-sequence stars with Pop. I chemical composition (X = 0.70, Z = 0.02) for three different values of k, i.e. $k = 1$ (full line), $k = 0.5$ (dashed line) and $k = 2$ (dotted line). Fig. 7 shows two important properties of low-mass stars: The first one is that a significant superadiabatic convection zone exists only in stars with a mass $M \gtrsim 0.65{\rm M}_\odot$. Below $M \approx 0.6{\rm M}_\odot$ the stratification is essentially adiabatic up to the photosphere. This means that application of our simple one-zone model is restricted to stars in the mass range $0.65{\rm M}_\odot \lesssim M \lesssim 1{\rm M}_\odot$. The second property shown in Fig. 7 is that the run of $T_{\rm B}(M)$ for different k is qualitatively the same for all three values of k. This means that as long as a star has a significant superadiabatic convection zone the transition from convective to radiative energy transport occurs in a rather narrow temperature interval, thus justifying our simple approach.

5.2. Stars with a mass $M \lesssim 0.6M_\odot$

As Fig. 7 shows, $T_{\rm B} \approx T_0$ in stars with a mass $M \lesssim 0.6{\rm M}_\odot$. This means on the one hand that the total optical depth between the photosphere (at $T = T_0$) and the point where $T = T_{\rm B}$ is small, in fact too small for our simple one-zone model, which assumes the diffusion approximation (Eq. 61), to be applicable. On the other hand, this means also that in these stars even in the photosphere a non-negligible fraction of the flux is transported by convection. Therefore, we must ask how irradiation changes the transported flux if the top of the (adiabatic) convection zone is at low optical depth. Because the convective flux is $F_{\rm conv} \sim (\nabla - \nabla_{\rm a})^{3/2}$ and the value of ∇ is directly influenced by irradiation, this situation cannot be described by a simple model. Rather one ought to determine ∇ by solving the full set of equations describing convective energy transport, i.e. in the simplest case the equations of mixing length theory. Considering the uncertainties inherent in current convection theories it is not obvious whether it is possible to make general statements about the functions g or G. After all it is at least conceivable that already a small irradiating flux could result in a significant reduction of $(\nabla - \nabla_{\rm a})$ (which itself is a rather small number because convection is not far from adiabatic) and that therefore $\partial F/\partial F_{\rm irr}$ could attain a large negative value. However, as the following argument shows, there is a limit to how fast F can drop in response to increasing $F_{\rm irr}$. If F drops too strongly this results in an effective temperature $T_{\rm irr} < T_0$. This in turn means that the temperature gradient must be steeper than in the unirradiated star and, therefore, that $F > F_0$, in contradiction to the starting assumption $\partial F/\partial F_{\rm irr} < 0$. In order to avoid this contradiction $T_{\rm irr}$ must not decrease with increasing $F_{\rm irr}$, i.e. $\partial T_{\rm irr}/\partial F_{\rm irr} \geq 0$, from which we immediately recover (33), i.e. $g \leq 1$. Because $g' < 0$ (cf. 34), g is maximal in the limit $F_{\rm irr} \to 0$. Therefore we need to determine $g(0)$ for the stars in question. For this we return to the one zone model (Sect. 5.1). From Eq. (69) we find that $g(0)$ increases as $T_{\rm B}/T_0$ decreases. In fact, in the limit $T_{\rm B} = T_0$, this model yields $g(0) = 1$. Thus the closer the adiabatic convection zone reaches to the surface the more sensitive the star is to irradiation, i.e. the larger g. On the other hand, we know that $g \leq 1$ in all cases. It is therefore plausible that for stars which are almost adiabatic up to the photosphere, i.e. $M \lesssim 0.6{\rm M}_\odot$, $g(0) \lesssim 1$. As we shall see below this is confirmed by numerical computations.

5.3. Results of numerical computations

Numerical computations of $g(x)$ and $G(x)$ have been carried out by HR97 for low-mass main sequence stars of Pop. I chemi-

cal composition using a full 1D stellar structure code (Hameury 1991), where the outer boundary condition was changed according to Eqs. (27) and (28) with $F_{\rm irr} = \text{const}$. The results relevant for this paper are shown in Fig. 8 and can be summarized as follows:

a) With $T_{\rm B}(M)$ as shown in Fig. 7 and an appropriately chosen value for b, i.e. $b \approx 4$–5, typical for H^- opacity, the predictions of our simple one-zone model are in good agreement with numerical results as long as $T_{\rm irr} < T_{\rm B}$. In particular, the run of $g(0)$ shown in Fig. 8 as a full line for the numerical computations and as a short-dashed line for the one-zone model show that within its range of validity the latter reproduces the numerical results quite well.
b) $g(0) \approx 1$ for stars with a mass $M \lesssim 0.5\mathrm{M}_\odot$, as we have argued above (Sect. 5.2).
c) $\mathrm{Max}(xg(x)) \lesssim 0.5$ over the whole mass range of interest, i.e. $0.1\mathrm{M}_\odot \lesssim M \lesssim 1\mathrm{M}_\odot$. This is shown as a dash-dotted line in Fig. 8.
d) In the point source model (cf Sect. 4.2.2) the integral $I_{\rm PS}$ in (57) has a maximum which is smaller than $(1 - f_{\rm s})$ $\mathrm{Max}(xg(x))$. $\mathrm{Max}(I_{\rm PS})$ is shown in Fig. 8 as a long dashed line. As can be seen, $\mathrm{Max}(I_{\rm PS}) \approx 0.20$.

6. Secular evolution with irradiation

We resume the stability discussion of Sect. 4, but now with the knowledge of the function $g(x)$ which we have gained in Sect. 5. We shall restrict most of the following to the constant flux model (Sect. 4.2.1) and the point source model (Sect. 4.2.2). In addition, we shall assume that all the properties of a binary along a secular evolution without irradiation, in particular the functions Γ and Λ defined respectively in Eqs. (41) and (45), are known. Among the compact binaries we specifically discuss cataclysmic variables, and low-mass X-ray binaries. In particular, we wish to examine the following questions: a) which systems are stable (unstable) at 1) turn-on of mass transfer, or 2) during the secular evolution, against irradiation-induced runaway mass transfer, and b) what kind of evolution do systems undergo which are unstable? Because part of these questions have been dealt with extensively by King (1995), KFKR95, KFKR96, KFKR97 and MF98, we shall mainly be concerned with those aspects which have not already been treated in detail in the above papers.

6.1. Cataclysmic variables

In the following we set $M_{\rm c} = M_{\rm WD}$ and $R_{\rm c} = R_{\rm WD}$, where $M_{\rm WD}$ and $R_{\rm WD}$ are respectively the mass and the radius of the accreting white dwarf. Furthermore we shall restrict our discussion to CVs where the secondary is a low-mass main sequence star. Because this is the case for the vast majority of CVs this is not a very strong restriction. For determining the values of Λ and Γ we adopt the standard evolutionary scheme for CVs, i.e. the model of disrupted magnetic braking (e.g. King 1988 for a review) and use results of corresponding model calculations by KR92.

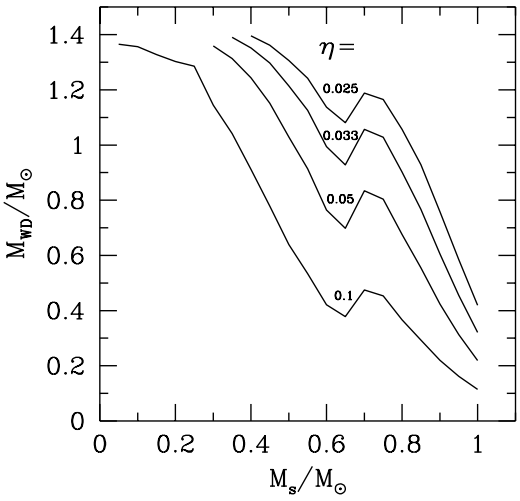

Fig. 9. Contour lines in the $M_{\rm WD} - M_{\rm s}$-plane along which $\zeta_{\rm irr}(F_{\rm irr} = 0) = 1$ for different values of η. Systems above (below) a particular line are unstable (stable) against irradiation-induced runaway mass transfer at the turn-on of mass transfer.

6.1.1. Stability of mass transfer at turn-on

Because $g(x)$ is maximal for $x = 0$, systems are most susceptible to irradiation at turn-on of mass transfer. The relevant stability criterion for the constant flux model is (51) and for the point source model Eq. (58). As we have already pointed out in Sect. 4 these conditions are in fact conditions on the efficiency factor η because everything else is basically fixed. Given the masses of both binary components, i.e. $M_{\rm WD}$ and $M_{\rm s}$, $R_{\rm WD}$ follows from the mass radius relation of white dwarfs, the secondary's radius $R_{\rm s}$ from the mass radius relation of main sequence stars, or from the evolutionary history. The orbital separation a follows from Roche geometry via $R_{\rm s}$ and the mass ratio, ζ_S and $\mathcal{F}$ from the secondary's internal structure, and finally $\zeta_{\rm R}$ again from the mass ratio. Thus Γ (Eq. 45) is uniquely determined by $M_{\rm WD}$ and $M_{\rm s}$. Given the function $g(x)$, and in particular $g(0)$, condition (51) is one for ηs, and condition (58) one for η only. Taking as an example g from our one-zone model with $b = 4$, $s = 0.5$ and $T_{\rm B}/T_0$ for $k = 1$ from Fig. 7, we can plot a line for a given η in the $M_{\rm s}$-$M_{\rm WD}$ plane along which mass transfer is marginally stable. This is shown in Fig. 9 for various values of η. The figure is to be read as follows: a parameter combination ($M_{\rm WD}$, $M_{\rm s}$) corresponds to a point in Fig. 9. If that point lies above the line corresponding to a given value of η, mass transfer is unstable at turn-on. What we can infer from Fig. 9 is that for typical WD masses $M_{\rm WD} \gtrsim 0.5\mathrm{M}_\odot$, condition (51) is violated for surprisingly small values of η, i.e. $\eta \lesssim 0.1$. This is the case, in particular, if $M_{\rm s} \gtrsim 0.6\mathrm{M}_\odot$. If we take instead of (51) the condition of the point source model (58), s is no longer a parameter. Taking again the same g as above (one-zone model with $b = 4$) the result is qualitatively the same. The main difference is that the value of η necessary for marginal stability needs to be larger by about a factor of 2.

The trends seen in the curves of Fig. 9 are easily explained: they reflect the run of $\Gamma(M_{\rm WD}, M_{\rm s})$ (cf Eq. 46). The smaller

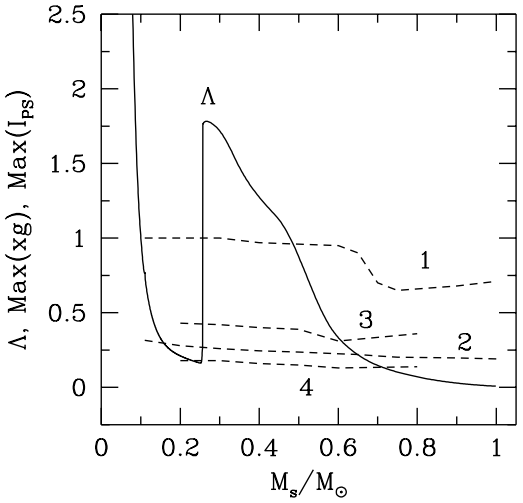

Fig. 10. The functions Λ (Eq. 41) (full line), $\mathrm{Max}[xg(x)]$ and $\mathrm{Max}(I_{\rm PS})$ according to the one-zone model (dashed lines 1 and 2 respectively), and $\mathrm{Max}[xg(x)]$ and $\mathrm{Max}(I_{\rm PS})$ derived from the results of HR97 (dashed lines 3 and 4 respectively) as a function of the secondary's mass along a standard evolution of a CV with $M_{\rm WD} = 1\mathrm{M}_\odot$ and $M_{\rm s,i} = 1\mathrm{M}_\odot$ calculated by KR92.

Γ the less stable mass transfer. Because Γ is proportional to $R_{\rm WD}/M_{\rm WD}$ and $\mathcal{F}^{-1}$, and $R_{\rm WD}/M_{\rm WD}$ is a steeply decreasing function of $M_{\rm WD}$ whereas $\mathcal{F}^{-1} \sim M_{\rm ce}/M_{\rm s}$ scales roughly as the relative mass of the convective envelope (cf. Fig. 1, dashed line) and thus decreases strongly with $M_{\rm s}$, mass transfer is more likely to be unstable (stable) the higher (lower) $M_{\rm WD}$ and $M_{\rm s}$. The other factors entering Γ, i.e. $(\zeta_S - \zeta_{\rm R})$, $M_{\rm s}/R_{\rm s}$ and $(a/R_{\rm s})^2$ are of comparatively minor importance. The fact that the curves in Fig. 9 are not monotonic results from the steep increase of $T_{\rm B}/T_0$ with stellar mass near $M = 0.65\mathrm{M}_\odot$ (cf. Fig. 7).

Because $g'(x) < 0$, systems in which mass transfer is stable at turn on will also be stable against irradiation-induced runaway mass transfer for any finite value of $F_{\rm irr}$, i.e. $\dot{M}_{\rm s}$. The opposite, however, is not true: not all systems which are unstable at turn-on will be so for the secular mean mass transfer rate.

6.1.2. Stability of secular evolution

The appropriate stability criterion is (41) in its most general form, (50) for the constant flux model and (57) for the point source model. Again, the left-hand side Λ of these criteria is fully determined by the adopted model of secular evolution, whereas the value of the corresponding right-hand sides still depends on η. As we have stressed in Sect. 4, we can give a sufficient criterion for stability of mass transfer because the function $xg(x)$ has a maximum. The corresponding criterion is (43) in its most general form,

$$\Lambda > 2s\ \mathrm{Max}(xg(x)) \tag{70}$$

for the constant flux model, and

$$\Lambda > \mathrm{Max}(I_{\rm PS}) \tag{71}$$

for the point source model. Conditions (70) and (71) can be read off Fig. 10 where we plot Λ as a function of secondary mass $M_{\rm s}$ (full line) along a standard secular evolution of a CV with $M_{\rm WD} = 1\mathrm{M}_\odot$ and an initial secondary mass $M_{\rm s,i} = 1\mathrm{M}_\odot$. The evolutionary data are taken from KR92. Into the same figure we plot $\mathrm{Max}(xg(x))$ $(= 2s\ \mathrm{Max}(xg(x))$ for $s = 1/2)$ and $\mathrm{Max}(I_{\rm PS})$ using results by HR97 for $g(x)$ (dashed lines). As can be seen the values of $\mathrm{Max}(xg(x))$ and $\mathrm{Max}(I_{\rm PS})$ are almost independent of secondary mass, i.e. of the orbital period. For CVs above the period gap, i.e. with $M_{\rm s} \gtrsim 0.25\mathrm{M}_\odot$, Λ increases very steeply with decreasing secondary mass. This behaviour is mainly due to two factors, first to $\mathcal{F}^{-1} \sim M_{\rm ce}/M_{\rm s}$ which increases strongly with decreasing mass, and second to $\tau_{\rm KH}$ which increases strongly towards lower masses mainly because of the mass luminosity relation $L \sim M^3$ of low-mass main sequence stars. So, what Γ essentially represents is the thermal inertia of the convective envelope. As can be seen from Fig. 10, the intersection of Λ with $\mathrm{Max}(xg(x))$ or $\mathrm{Max}(I_{\rm PS})$ is near $M_{\rm s} = 0.7\mathrm{M}_\odot$. Because Λ increases so steeply, small changes in $\mathrm{Max}(xg(x))$ or $\mathrm{Max}(I_{\rm PS})$ do not yield a significantly different result.

When a CV approaches the period gap, i.e. the secondary becomes fully convective at $M_{\rm s} \approx 0.25\mathrm{M}_\odot$, the system detaches and $\Gamma \to 0$ because $\tau_{M_{\rm s}} \to \infty$. When mass transfer resumes Λ is smaller by typically a factor 10 than immediately above the gap, reflecting the reduced angular momentum loss below the gap and the fact that at turn-on $R_{\rm s} = R_0$ (cf. 41). Λ starts increasing again with further decreasing mass because the Kelvin-Helmholtz time $\tau_{\rm KH}$ becomes very long as the secondary becomes degenerate.

Because Λ does not depend strongly on the mass of the white dwarf we can generalize the result found from Fig. 10: In the framework of standard CV evolution, i.e. the model of disrupted magnetic braking, CVs are stable against irradiation-induced runaway mass transfer when the mass of the secondary star is $M_{\rm s} \lesssim 0.7\mathrm{M}_\odot$. If, on the other hand, $M_{\rm s} \gtrsim 0.7\mathrm{M}_\odot$, a system can be unstable but need not be so, subject to the value of η.

We note, however, that by invoking substantial consequential angular momentum loss (CAML), i.e. angular momentum loss which depends explicitly on the mass transfer rate (see King & Kolb 1995 for a discussion of CV evolution with CAML), the mass range over which systems can be unstable is much larger. This has already been pointed out by KFKR96 and confirmed in computations by MF98.

As can be seen in Fig. 10 there is also a slight chance that CVs immediately after turn-on below the period gap are unstable. According to the constant flux model (Eq. 72), some CVs could be unstable, according to the point source model, which is more realistic but still very optimistic, the stability criterion (71) is violated only marginally if at all. Therefore, our conclusion is that CVs below the period gap are very probably stable, at least in the framework of standard CV evolution.

Examining the factors which determine the value of Λ (Eq. 41) we see that within a given evolutionary model all factors are determined. ζ_S, $\tau_{\rm KH}$ and $\mathcal{F}$ depend only on the mass of the

secondary and its evolutionary history, τ_{M_s} on the adopted rate of angular momentum loss, $\zeta_S - \zeta_R$ and the evolutionary history (via $(\partial \ln R_s/\partial t)_{th}$ in (3)), ζ_R on the mass ratio and R_s/R_0 on the evolutionary history (e.g. Stehle et al. 1996). We see also that making Λ smaller (in order to get the instability for lower secondary masses) is possible only by either increasing τ_{M_s}, i.e. lowering the mean mass transfer rate $\langle \dot{M}_s \rangle$, or by increasing ζ_R. The former is practically impossible without upsetting the standard evolutionary paradigm for CVs, i.e. the period gap model which requires that above the period gap ($M_s \gtrsim 0.25 M_\odot$, $P \gtrsim 3^h$) $\tau_{KH}/\tau_{M_s} \gtrsim 5$ (e.g. Ritter 1984, King 1988; KR92; Stehle et al. 1996). Increasing ζ_R, on the other hand, is possible only if a system experiences significant CAML.

6.2. Low-mass X-ray binaries

At first glance one might suspect that in LMXBs irradiation of the secondary represents a much larger threat for the stability of mass transfer than it does in CVs. However, for the following reasons this is very probably not the case: first we note the observational fact that very few of the LMXBs show X-ray eclipses. This has been interpreted as a consequence of the large vertical scale height of the X-ray irradiated accretion disk. This in turn allows the secondary to stay permanently in the disk's shadow. If this is the case, none or at most a small part of the secondary's surface is directly exposed to the accretion light source. Second, indirect illumination of significant parts of the donor (the high latitude regions or part of the back side) is ruled out because this would require a very extended scattering corona indeed, with a typical size of the scattering sphere (at optical depth $\tau \sim 1$) of order or larger than the donor star. As a consequence one would expect X-ray eclipses to occur much more frequently than they are actually observed. Third, heat transport by currents from the hot, illuminated to the cool parts in the X-ray shadow are probably also negligible. This is because in cool stars with a deep convective envelope the superadiabatic convection zone isolates the interior from the surface. It is itself unable to transport significant amounts of heat because of its small heat capacity and the fact that the thermal time scale is much shorter than the time scale of circulation.

Heat transport by currents caused by hydrostatic disequilibrium is, however, of importance in stars with a radiative envelope. Effects of this are e.g. seen in the X-ray binaries HZ Her and V1033 Sco (see e.g. Shahbaz et al. (2000), and references therein).

Because neither indirect llumination nor heat advection can contribute significantly to the blocking of the stellar flux, the integral I on the right-hand side of (41) is much smaller than for a comparable CV, despite the fact that in a LMXB there is potentially much more energy available for irradiating the secondary. The fact that $xg(x)$ has a maximum at $x \approx 1$ is the reason why even large irradiating fluxes do not help. Rather, optimal irradiation is achieved if as large a fraction as possible of the secondary's surface is irradiated with a flux such that $xg(x)$ is near its maximum, i.e. if $x \approx 1$. This is clearly not the case in LMXBs. Not only is the surface fraction which is directly irradiated small, worse, where the surface of the secondary is directly exposed to the X-ray source, the associated flux is large, i.e. $x \gg 1$ unless η is assumed to be very small. The latter is very unlikely considering the fact that most of the accretion luminosity emerges in form of rather hard X-rays. Thus, unless the secular evolution of LMXBs is totally unlike that of CVs as far as the nature of the secondary and the typical mass transfer rates are concerned, the value of Λ is virtually the same as for CVs but, as explained above, the right-hand side of (41) is much smaller than in CVs. Therefore we conclude that very probably LMXBs are stable against this type of irradiation-induced runaway mass transfer. As has been noted by KFKR97, systems in which accretion is intermittent rather than continuous, i.e. transient LMXBs, are even more stable.

6.3. Evolution of unstable systems

Let us now discuss briefly the evolution of systems (i.e. CVs) in which the stationary mass transfer given by (3) is unstable, i.e. systems for which the stability criterion (41) or a special form thereof (Eqs. 50 or 57) is violated. From the fact that $g'(x) < 0$ we know that mass transfer is then already unstable at turn-on. Therefore, when mass transfer turns on, the mass transfer rate increases, and because (41) is violated, it does not settle at the secular mean $\langle -\dot{M}_s \rangle$ given by (3). However, because the thermal relaxation caused by irradiation saturates both in amplitude and with time (see our discussion in Sect. 3, in particular Eqs. (20) and (23), and Fig. 4) the mass transfer rate does not run away without bound. Rather, there is an upper limit: with (20) we obtain for the maximum mass transfer rate

$$\begin{aligned} \mathrm{Max}(-\dot{M}_s) &\approx \langle -\dot{M}_s \rangle + \frac{M_s}{(\zeta_S - \zeta_R)}\ \mathrm{Max}\left\{\frac{s_{\rm eff}}{\tau_{KH}}\,\mathcal{F}\right\} \\ &\approx \langle -\dot{M}_s \rangle + \frac{s}{\zeta_S - \zeta_R}\frac{M_s}{\tau_{KH}}\,\mathcal{F} \quad . \end{aligned} \tag{72}$$

Because mass transfer can be unstable against irradiation only if $M_s \gtrsim 0.7 M_\odot$, i.e. when the secondary has a relatively thin convective envelope and thus $\mathcal{F}$ is large (cf. Fig. 1), the maximum contribution of irradiation to mass transfer can be several times ($s\mathcal{F}$ times) the thermal time scale mass transfer rate M_s/τ_{KH}. Thus, for such systems $\mathrm{Max}(-\dot{M}_s) \gg \langle -\dot{M}_s \rangle$.

After having reached the peak mass transfer rate, mass transfer cannot continue at that rate. Rather it must decrease with time for two reasons: first, thermal relaxation saturates on the time scale given by (23), i.e. $(\partial \ln R/\partial t)_{irr}$ decreases on that time scale. Second, because mass transfer occurs at a rate above the secular mean, the binary system is driven apart, i.e. $(d \ln R_R/dt) > (d \ln R_s/dt)$. Both effects result eventually in the termination of mass transfer. The system becomes slightly detached, the secondary, in the absence of irradiation, shrinks. However, because of the absence of mass transfer the contraction of the system due to angular momentum loss is fast enough to catch up, so that mass transfer resumes and the cycle repeats again. In other words: if a system is unstable at the secular mean mass transfer rate it must undergo a limit cycle in which phases of enhanced, irradiation-driven mass transfer alternate with phases of very

low or no mass transfer. The conditions for the occurrence of mass transfer cycles in semi-detached binaries have been investigated in more detail and using more general principles (in the framework of non-linear dynamics) by King (1995), KFKR95, KFKR96 and KFKR97. Their main result is that mass transfer cycles driven by radius variation of the secondary can only occur if $(\partial \ln R_{\rm s}/\partial t)_{\rm th}+(\partial \ln R_{\rm s}/\partial t)_{\rm nuc}$ in (1) depends explicitly on the *instantaneous* mass transfer rate. The only plausible mechanism providing such a dependence is irradiation of the donor star by radiation generated through accretion, i.e. the situation we are studying in this paper. The necessary criterion for the occurrence of mass transfer cycles found by these authors is identical to what we have found here, namely the violation of (41). In the framework of a linear stability analysis of mass transfer, with which we, King (1995), KFKR95, KFKR96 and KFKR97 have been concerned so far, we can not calculate the long-term evolution over time scales $\tau_{M_{\rm s}}$ of systems under the irradiation instability. For this the full set of equations describing mass transfer and stellar structure under irradiation have to be solved. Results of such calculations and computational details will be presented in the following section. Because similar computations have already been done by HR97 and MF98, we shall concentrate here on aspects which have not been dealt with in detail by HR97 and MF98, but are, in our opinion, important for better understanding of the evolution under the irradiation instability.

7. Secular evolution with irradiation: numerical computations

7.1. Computational techniques

To compute the secular evolution of a compact binary with a low-mass donor star we have used the bipolytrope programme described in detail in KR92. With respect to the procedure described in KR92 we have, however, implemented two modifications in order to allow for a proper treatment of irradiation and its consequences for the secular evolution.

First, we compute the mass transfer rate explicitly rather than by using Eq. (3) as in KR92, i.e. we adopt the following prescription (e.g. Ritter 1988):

$$-\dot{M}_{\rm s} = \dot{M}_0 \exp\left[-\frac{R_{\rm R}-R_{\rm s}}{H_{\rm P}}\right] \tag{73}$$

Expressions for the photospheric pressure scale height $H_{\rm P}$ and the factor $\dot{M}_0$ in terms of stellar parameters of the donor star and binary parameters are also given in Ritter (1988). In the context of this paper the donor star is always a low-mass main sequence star. For such stars both, $H_{\rm P}$ and $\dot{M}_0$ are only weak functions of the stellar mass and have typical values $H_{\rm P}/R_{\rm s} \approx 10^{-4}$ and $\dot{M}_0 \approx 10^{-8}{\rm M}_\odot\ {\rm yr}^{-1}$. The reason for using (73) instead of (3) is that the latter is valid only for stationary mass transfer. However, this is not a good approximation when a system evolves through mass transfer cycles, because such cycles proceed unavoidably through phases of non-stationary mass transfer. In order to simplify the computation of $-\dot{M}_{\rm s}$ we used fixed values for $H_{\rm P}$ and $\dot{M}_0$, i.e. $H_{\rm P} = 10^{-4}R_{\rm s}$ and $\dot{M}_0 = 10^{-8}{\rm M}_\odot\ {\rm yr}^{-1}$. Furthermore we used (73) also when $-\dot{M}_{\rm s} > \dot{M}_0$, i.e. when the donor star overfills its critical Roche volume. (73) is still a reasonable approximation if $R_{\rm s}-R_{\rm R} <$ few $H_{\rm P}$, i.e. $-\dot{M}_{\rm s} \lesssim 10^{-7}{\rm M}_\odot\ {\rm yr}^{-1}$ (see e.g. Kolb & Ritter 1990) which is adequate for our purposes.

When computing the mass transfer rate from (73) we use for $H_{\rm P}$ and $\dot{M}_0$, both of which depend on the effective temperature, the value of $T_{\rm eff}$ on the unirradiated part of the star, i.e. $T_{\rm eff} = T_0$. There are two main arguments for this choice: first, in disk-accreting systems the inner Lagrangian point L_1 is in the shadow of the disk and the cooling time of gas in the superadiabatic layer flowing from the irradiated parts towards L_1 is short compared to the flow time in the shadow region. Second, if we use $T_{\rm eff} = T_{\rm irr}$ instead of $T_{\rm eff} = T_0$, $H_{\rm P}$ and $-\dot{M}_{\rm s}$ would react practically instantaneously and with a large amplitude to irradiation giving, in turn, rise to a runaway of the mass transfer rate on an extremely short time scale (order of hours). This is obviously not what happens in the systems we do observe.

Second we use either Eq. (52) in the constant flux model or Eq. (59) in the point source model of irradiation in place of the usual Stefan-Boltzmann law as one of the outer boundary conditions for the donor star model. For the calculations presented below we have used the one-zone model described in Sect. 5 rather than results obtained from full stellar models by HR97 described earlier. Specifically, $T_{\rm irr}$ in (52) or (59) was computed by solving (68) in which $F_{\rm irr}$ is determined for an adopted value of η from (24) with $h(\vartheta,\varphi)$ taken respectively from (48) and (49) in the case of the constant flux model, and from (54) in the case of the point source model. $T_{\rm B}$ in (68) is taken from the numerical results shown in Fig. 7. Specifically, we have used $T_{\rm B}(M_{\rm s})$ for $k = 1$. Furthermore, in order to determine $T_{\rm irr}$ we need to specify b, i.e. the temperature exponent of the photospheric opacity law (10). For most of our experiments we have used $b = 4$ which is adequate for H^- opacity.

The diagnostic quantities $\zeta_{\rm irr}$ and $s_{\rm eff}$ are calculated from (44) and respectively (53) or (60) with the appropriate choice of $h(\vartheta,\varphi)$, i.e. Eqs. (48) or (54), and $g(\vartheta,\varphi)$ from (69).

7.2. Computational limitations

By using the bipolytrope approximation for describing the internal structure of the donor star, we can only deal with chemically homogeneous stars which have a radiative core and a convective envelope or are fully convective, i.e. with low-mass ($M_{\rm s} \lesssim 1{\rm M}_\odot$) zero age main sequence stars. Thus, we are unable to address chemically evolved stars, in particular subgiants. Giants, on the other hand, have been dealt with approximately by KFKR97. We note also that chemically evolved donors among CVs might be more common than hitherto thought (Kolb & Baraffe 2000; Ritter 2000; Baraffe & Kolb 2000) and therefore deserve further study. For our computations, we have adopted Pop. I chemical composition. In the context of the bipolytrope approximation, the chemical composition is of relevance mainly for determining the appropriate gauge functions, i.e. polytropic index n_1 of the radiative core and entropy jump h in the surface layers as a function of stellar mass (for details see KR92). Even when adopting the appropriate gauge functions, we know that

the value of ζ_S computed in the bipolytrope approximation is smaller than what one would obtain for a full stellar model if $M \gtrsim 0.6\mathrm{M}_\odot$. Because of this, in the bipolytrope approximation binary systems are more likely to be unstable against irradiation than they are in reality if $M_\mathrm{s} \gtrsim 0.6\mathrm{M}_\odot$.

We have used the one-zone model described in Sect. 5. As we have discussed there, application of this model is practically restricted to stars with a mass $M_\mathrm{s} \gtrsim 0.6$–$0.7\mathrm{M}_\odot$. We have, however, carried out a few calculations of systems with a smaller secondary mass. In those cases we have assumed $g(x) = 1$ if $0 \le x \le 1$ and $g = 0$ otherwise. This corresponds to what (69) yields in the limit $T_\mathrm{B} \to T_0$ and approximates results of numerical calculations, at least for small fluxes, i.e. $x < 1$, reasonably well.

Our calculations contain a number of free or at best not well-constrained parameters. To mention just the most important ones: in the constant flux model we already make a very simplifying assumption about the function $h(\vartheta, \varphi)$, i.e. the irradiation geometry. This assumption results in the free parameter s. In addition, we have the efficiency factor η, a parameter about which we know little beyond the fact that probably $0 < \eta \lesssim 1$. Using our one-zone model (Sect. 5) introduces furthermore the parameters T_B and b, both of which can, however, be fixed reasonably well by comparison with full stellar models. In the point source model we do not need to specify s. But all the other parameters, i.e. η, T_B and b remain in the problem. By using numerical results for the functions $G(x)$ and $g(x)$ we would get rid of the parameters T_B and b. But we would still be left with specifying $h(\vartheta, \varphi)$ and η. On top of all that we have also a number of input parameters and functions which are already needed for computing a secular evolution without irradiation. Apart from the binary's initial parameters the most important of those are the angular momentum loss rate and parameters arising from assumptions about mass and consequential angular momentum loss from the binary system.

The purpose of the following computations, going beyond the linear stability analysis, is to illustrate the temporal evolution under the irradiation instability and a number of its specific properties which we have uncovered in the foregoing discussion.

As we have demonstrated in the previous section the irradiation instability is more likely of relevance for CVs than for LMXBs. Consequently, in the examples below we have assumed that the accretor is a white dwarf with a mass $M_\mathrm{WD} = 1\mathrm{M}_\odot$ and a radius according to the mass radius relation (e.g. Nauenberg 1972) of $R_\mathrm{WD} = 5\ 10^8$cm. We assume that during the secular evolution the mass of the white dwarf remains constant, i.e. $\langle \dot{M}_\mathrm{WD} \rangle = 0$, and that on average the transferred matter leaves the system with the specific orbital angular momentum of the white dwarf. Other parameters characterizing the three examples which we shall discuss subsequently in detail are listed in Table 2.

7.3. Numerical results

For the first example of a secular evolution with irradiation, results of which are shown in Fig. 11, we have adopted the constant flux model with $s = 0.5$, an initial secondary mass $M_\mathrm{s,i} = 0.8\mathrm{M}_\odot$ and loss of orbital angular momentum on a constant time scale $\tau_J = -J/\dot{J} = 1.27\ 10^8$ yr derived from the Verbunt & Zwaan (1981) prescription for magnetic braking with $f_\mathrm{VZ} = 1$. The value $\eta = 0.035$ was chosen such that on the one hand initially $\zeta_\mathrm{irr} > \zeta_S - \zeta_\mathrm{R}$ and on the other $T_\mathrm{irr} < T_\mathrm{B}$ at all times. The top panel of Fig. 11 shows the run of the mass transfer rate with irradiation (full line) and without (dashed line), the second the evolution of the secondary's radius

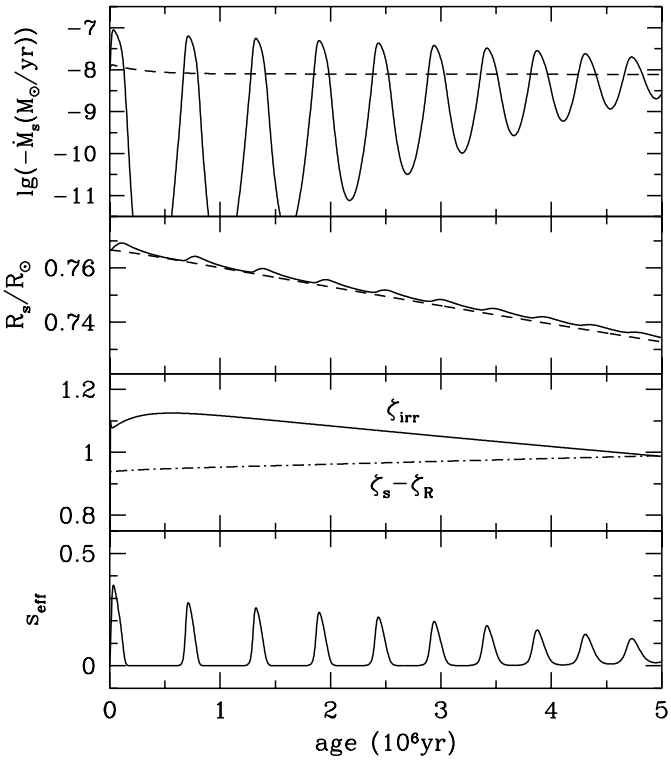

Fig. 11. Evolution of a CV with an initial secondary mass $M_\mathrm{s,i} = 0.8\mathrm{M}_\odot$ through mass transfer cycles computed by adopting the constant flux model with $s = 0.5$ and the one-zone model with $b = 4$. Further parameters and model assumptions are listed in Table 2. Shown as a function of time are: in the top frame the mass transfer rate with and without taking into account the effect of irradiation (full and dashed line respectively); in the second frame the secondary's radius with and without taking into account the effect of irradiation (full and dashed line respectively); in the third frame ζ_irr according to Eq. (40)(full line) and $\zeta_S - \zeta_\mathrm{R}$ (dashed line); in the bottom frame s_eff according to Eq. (53).

Table 2. Parameters and model assumptions used for calculating the evolution shown in Figs. 11–13. Parameters common to all three examples are: $M_\mathrm{WD} = 1\mathrm{M}_\odot$, $R_\mathrm{WD} = 5\,10^8$ cm, $H_\mathrm{P}/R = 10^{-4}$, $\dot{M}_0 = 10^{-8}\mathrm{M}_\odot\mathrm{yr}^{-1}$; irradiation model: one-zone model with $b = 4$; irradiation geometry: constant flux over surface fraction $s = 0.5$.

parameter	value		
	Fig. 11	Fig. 12	Fig. 13
$M_\mathrm{s,i}(\mathrm{M}_\odot)$	0.80	0.70	0.25
η	0.035	0.035	0.20
$\tau_J(\mathrm{yr})$	$1.27\,10^8$	$1.27\,10^8$	$2.95\,10^9$

with irradiation (full line) and without (dashed line). In the third panel we show the run of $\zeta_{\rm irr}$ (full line) and of $\zeta_S - \zeta_{\rm R}$ (dash-dotted line) with time. Finally the bottom panel shows the run of $s_{\rm eff}$ with time. As was to be expected for a system in which (initially) $\zeta_{\rm irr} > \zeta_S - \zeta_{\rm R}$ mass transfer evolves through cycles with at least initially large amplitude. The amplitude of the radius variations, on the other hand, are small, a consequence of the small value of $H_{\rm P}/R = 10^{-4}$. According to (73) we have $\Delta \log R_{\rm s} = H_{\rm P}/R\ \Delta \log \dot{M}_{\rm s}$. We see also that during the mass transfer peaks a significant fraction of the stellar luminosity is blocked. Because η has been chosen such that always $T_{\rm irr} < T_{\rm B}$ we always have $s_{\rm eff} < s$. What is immediately apparent from this calculation is that though the system evolves through mass transfer cycles, these are damped on a rather short time scale, i.e. a time scale much shorter than τ_J. The reason for this is that $\zeta_{\rm irr}$ decreases rapidly with time (mass of the donor). Eventually $\zeta_{\rm irr} < \zeta_S - \zeta_{\rm R}$ and mass transfer becomes stable. This is mainly a consequence of the increasing thermal inertia of the convective envelope, i.e. of a decrease of $\mathcal{F}/\tau_{\rm KH}$ with decreasing donor mass. The damping of the oscillations could only be overcome if at the same time g increases sufficiently strongly with decreasing mass. We shall show below that in a restricted mass range this is indeed possible.

Given the results of the above example we now ask to what extent they are representative, i.e. whether the qualitative behaviour depends strongly on the adopted model parameters or not. With this end in view we have carried out numerous experiments, the results of which we shall now discuss.

Working with the one-zone model (Sect. 5) we ask first how the above results change with the parameter b, i.e. the adopted photospheric opacity. Inspection of Eq. (69) shows that for given values of $T_{\rm B}$ and $T_{\rm irr}$ $g(0)$ increases with b. This means that at least for small fluxes the donor star is more sensitive to irradiation for larger b. The reason for this is easy to understand: the larger b the more pronounced the increase of the optical depth in the superadiabatic layer in response to irradiation, i.e. of the average temperature, and thus the more effective the blocking of the energy outflow from the adiabatic interior. Thus, increasing (decreasing) b above (below) the value $b = 4$ we have used in the example shown in Fig. 11 results in more (less) pronounced mass transfer cycles. The time scale on which the mass transfer oscillations are damped remains, however, essentially unaffected by changes of b, reflecting the fact that $\mathcal{F}/\tau_{\rm KH}$ does not depend on b.

Next we compare the results obtained with the constant flux model (Fig. 11) with those obtained with the point source model. The results of a run with the latter model and parameters identical to those used for producing Fig. 11 (except of s which is not a free parameter in this model) are qualitatively very similar to those found in Fig. 11. The amount of stellar flux blocked during a mass transfer peak is, however, systematically smaller (by about a factor of two) than in the constant flux model. The main reason for this is that the irradiated area on the donor $s_{\rm PS} = 0.5(1 - f_{\rm s}) = 0.32$ is smaller by about a factor of 1.6 than what we have assumed in the constant flux example, i.e. $s = 0.5$. Therefore, in order to achieve the same effect as in the constant flux model with $s = 0.5$, η in the point source model needs to be increased by about a factor of two. Otherwise the results obtained from the two models are very similar. Because of this and because the constant flux model is computationally much less demanding we have performed most of our simulations with that model.

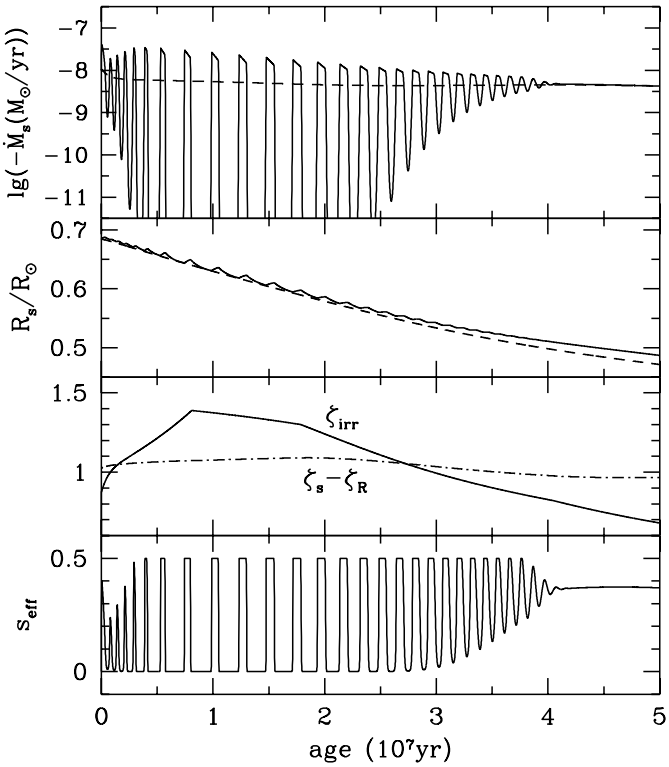

Fig. 12. As Fig. 11, but with an initial secondary mass $M_{\rm s,i} = 0.7{\rm M}_\odot$. Further parameters and model assumptions are listed in Table 2.

Next we examine briefly the dependence on the initial mass of the donor star. From our extensive discussions in Sects. 4 and 6 we know already that below a critical mass which is between about 0.6 and $0.7{\rm M}_\odot$, depending on the adopted models, systems following a standard CV evolution are stable against irradiation.

Adopting the constant flux model and the one-zone model, a system with an initial secondary mass of $0.7{\rm M}_\odot$ is still unstable (whereas with the point source model and a more realistic $g(x)$ such a system would be stable). Results of an evolution with $s = 0.5$ and $\eta = 0.04$ and the remaining parameters as in Fig. 11 (cf. Table 2) are shown in Fig. 12. As can be seen this evolution differs in several respects from the one shown in Fig. 11. Initially the amplitude of the mass transfer cycles increases with time. After only a few cycles the peak mass transfer rate is so high that the irradiation effect saturates, i.e. $T_{\rm irr} > T_{\rm B}$ and $s_{\rm eff} = s = 1/2$. Although the one-zone model used here does not apply when $T_{\rm irr}$ approaches $T_{\rm B}$, the main effect of saturation can be modelled anyway by setting $g = 0$ if $T_{\rm irr} \geq T_{\rm B}$. The qualitative behaviour obtained in this way remains the same as if a more realistic and smooth function $g(x)$ was used. After an initial phase of increasing amplitudes they later start decreasing

and die out very rapidly after about $4\,10^7$ yr. This behaviour can be understood as follows: We have already pointed out above that increasing amplitudes of the cycles can only be expected if with decreasing mass $g(x)$ increases fast enough. This is exactly what happens in the evolution shown in Fig. 12. The fast increase of $g(x)$ is the result of the fast decrease of $T_{\rm B}/T_1$ when going from $M_{\rm s} \approx 0.7{\rm M}_\odot$ to $M_{\rm s} \approx 0.6{\rm M}_\odot$ (see Fig. 7). Below $M_{\rm s} \approx 0.6{\rm M}_\odot$, $g(x)$ does no longer change much with mass. As a result, the mass transfer cycles are then damped because of the secular increase of $\tau_{\rm KH}/\mathcal{F}$. When the system eventually becomes stable, irradiation is still important in blocking the energy outflow. As can be seen from the bottom panel of Fig. 12, $s_{\rm eff}$ is of the order 0.37 after the system has stabilized.

Going to even lower initial secondary masses, mass transfer cycles cannot occur unless either $\zeta_S - \zeta_{\rm R}$ or $\langle \dot{M}_{\rm s} \rangle$ is much smaller than in a standard CV evolution (cf. our discussion in Sect. 6.1). For illustrating this we show in Fig. 13 the results of a calculation for which we have assumed $M_{\rm s} = 0.25{\rm M}_\odot$, $\eta = 0.20$, $s = 0.5$ and the much smaller angular momentum loss rate of gravitational radiation. Thus these parameters mimic an unstable system just below the period gap. As we have seen at the end of Sect. 6.1, CVs just below the period gap can be unstable if the constant flux model with $s = 0.5$ is adopted. They are, however, stable if the point source model is used, unless $\zeta_{\rm R}$ is lowered below the standard value by invoking CAML (see MF98). If we use in addition to the constant flux model also the one-zone model in the limit $T_{\rm B} \to T_1$, at low fluxes the donor star is even more susceptible to irradiation than if a more realistic form of $g(x)$ had been used. However, for the purpose of this exercise it does not matter whether CVs below the gap are stable or not. This example was chosen just to demonstrate that with a low enough $\langle -\dot{M}_{\rm s} \rangle$ and depending on the value of η a system could evolve through mass transfer cycles as we have concluded from our stability discussion in Sects. 4 and 6. One additional property of this run which is worth mentioning is that the cycles are only rather weakly damped. The reason for this is that a star with a mass $M_{\rm s} < 0.25{\rm M}_\odot$ is always fully convective and therefore $\mathcal{F} = 7/3$ remains constant. Thus the decrease of $\zeta_{\rm irr}$ is mainly due to the slow increase of $\tau_{\rm KH}$ with time.

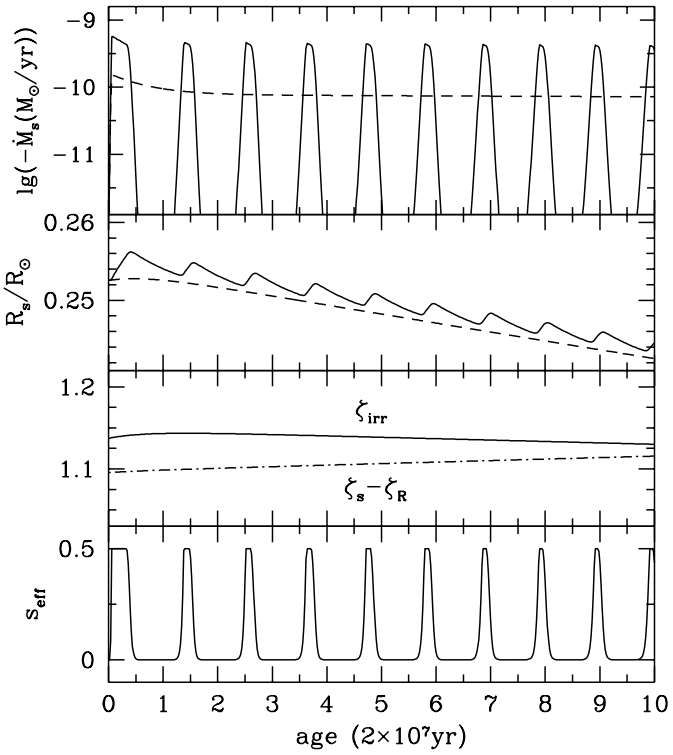

Fig. 13. As Fig. 11, but with an initial secondary mass $M_{\rm s,i} = 0.25{\rm M}_\odot$ and assuming orbital angular momentum loss only via gravitational radiation. Further parameters and model assumptions are listed in Table 2.

8. Discussion and conclusions

With the exception of the numerical examples presented in the previous section, where we have assumed the donor star to be on the ZAMS, we have so far not made any explicit assumption about the evolutionary status of the secondary. In fact our stability considerations are valid for any type of donor star as long as it has a sufficiently deep outer convective envelope. In the following we shall therefore briefly address the stability of mass transfer and the peak mass transfer rate in case of instability if the secondary is more or less nuclear evolved. In addition we shall briefly discuss the impact of the donor's metallicity on the stability of mass transfer. A detailed investigation of the irradiation instability in those cases is, however, deferred to a subsequent paper.

8.1. Effects of evolution and metallicity on the stability of mass transfer

Returning to the stability criterion (41) we see that the left-hand side Λ depends essentially only on the ratio of two time scales, i.e. the thermal time scale of the convective envelope $\tau_{\rm ce}$ and the mass transfer time scale $\tau_{M_{\rm s}}$ or, respectively, on the time scale on which mass transfer is driven $\tau_{\rm dr} = (2/\tau_J + 1/\tau_{\rm nuc})^{-1}$. Mass transfer is more stable the larger the ratio $\tau_{\rm ce}/\tau_{\rm dr}$.

Evolutionary computations such as those shown in Ritter (1994) show that at a given secondary mass $\tau_{\rm ce}$ is the shorter the more evolved the star. If magnetic braking according to Verbunt & Zwaan (1981) is invoked for computing the angular momentum loss rate, numerical computations (e.g. those shown in Ritter 1994, or King et al. (1996a) of the mass transfer from a nuclear evolved donor show that $\tau_{\rm dr}$ is the longer the more evolved the donor at the *onset* of mass transfer. Taken together this means that mass transfer is the more unstable (less stable) the more evolved the donor. As an example, evaluating Λ along the evolutionary tracks shown in Ritter (1994) we find that as long as the secondary has not reached the terminal age main sequence, mass transfer is stable if $P \lesssim 5^h - 6^h$. In the sequence starting with a $1.2{\rm M}_\odot$ secondary at the end of central hydrogen burning, systems down to an orbital period $P \approx 2^h$ may be unstable.

Main sequence stars of low metallicity are systematically hotter, smaller, more luminous and have a thinner convective envelope than main sequence stars of solar metallicity. Hence

$\tau_{\rm ce}$ is systematically shorter for low metallicity stars. At the same time $\tau_{M_{\rm s}}$ is the shorter the lower the metallicity. Taken together this means that mass transfer is systematically more unstable (less stable) the lower the metallicity. As an example, using results from Stehle et al. (1997), we find that in CVs with a Pop. II donor mass transfer could be unstable for orbital periods as low as $\sim 4^h$.

The case of systems containing a giant donor and in which mass transfer is driven by its nuclear evolution, i.e. $\tau_{\rm dr} = \tau_{\rm nuc}$, has already been dealt with in some detail by KFKR97. We shall mention here only that such systems are systematically more unstable against irradiation-induced runaway mass transfer than systems with a main sequence donor. There are three reasons for this: First, for a giant $\tau_{\rm ce}$ is systematically shorter than for a main sequence star of the same mass (because of the much larger values of R and L), and this despite the fact that $M_{\rm ce}/M$ can be quite large. Second, in terms of radius changes due to irradiation, giants react much more strongly than main sequence stars. (Note that in the framework of the homology model presented in Sect. 3 the effective ν for giants is -3). Third, the mass transfer time scale $\tau_{M_{\rm s}}$associated with nuclear evolution of a giant is always much longer than $\tau_{\rm ce}$ over the entire range of core masses of interest, i.e. $0.15{\rm M}_\odot \lesssim M_{\rm c} \lesssim 0.5{\rm M}_\odot$. For details see KFKR97 and Ritter (1999).

8.2. The peak mass transfer rate

Our estimate (72) of the peak mass transfer rate achieved during a mass transfer cycle can be rewritten as

$$\mathrm{Max}(-\dot{M}_{\rm s}) \approx \langle -\dot{M}_{\rm s}\rangle \left[1+\frac{2s}{\Lambda}\right] \quad . \tag{74}$$

In the case of a fully developed instability it is the second term in (74) which dominates. Therefore, the peak mass transfer rate is essentially determined by the rate of expansion of the donor, i.e.

$$\mathrm{Max}(-\dot{M}_{\rm s}) \approx \langle -\dot{M}_{\rm s}\rangle \frac{2s}{\Lambda} \approx \frac{M_{\rm s}}{\zeta_S-\zeta_{\rm R}}\frac{s}{\tau_{\rm ce}} \quad . \tag{75}$$

Thus the lower the thermal inertia of the convective envelope the higher the peak mass transfer rate. As a consequence, very high peak rates can result if the mass of the convective envelope or $\tau_{\rm KH}$ is small. If this is the case the long-term evolution of the corresponding systems could be drastically changed. We note e.g. that even if the donor is a main sequence star, the peak mass transfer rate can easily exceed the value required for maintaining stable nuclear burning on the white dwarf, i.e. $\dot{M}_{\rm WD} \gtrsim 10^{-7}{\rm M}_\odot{\rm yr}^{-1}$ (e.g. Fujimoto 1982). With a Pop. I ZAMS donor this limit is reached if $M_{\rm s} \gtrsim 0.8{\rm M}_\odot$ (see Fig. 11), with a donor at the end of central hydrogen burning if $P \gtrsim 10^h$ or $M_{\rm s} \gtrsim 0.6{\rm M}_\odot$. These values are derived from the evolutionary calculations discussed in Ritter (1994).

The consequences of reaching peak mass transfer rates equal to or even in excess of the stable nuclear burning limit of the white dwarf can be far-reaching. First, if steady nuclear burning on the white dwarf is reached, such a system will no longer appear as an ordinary CV but rather look more like a supersoft X-ray source. Because such systems are bright in the EUV only, they become virtually undetectable in our Galaxy: very few such systems have indeed been found (see e.g. Greiner 1996). Second, with nuclear burning on the white dwarf, the nuclear luminosity exceeds the accretion luminosity by a factor of $\sim$ 10–10^2. With so much more irradiation luminosity available effects other than those discussed in this paper might also become important, e.g. driving of a strong wind from the donor (see van Teeseling & King 1998, King & van Teeseling 1998), and which would change the evolution of such systems altogether. Third, an unavoidable consequence of the very high peak mass transfer rates are very extended low states during which a system is practically detached and thus virtually undetectable. Fourth, from the fact that such systems are barely detectable in both the high and low state and that the transition time between high and low states and vice versa is very short (see KFKR97), one is practically forced to the conclusion that the observed long-period CVs are either stable against the irradiation instability or, for some other reason do not reach peak rates equal to or larger than the stable nuclear burning limit.

8.3. Conclusions

In this paper we have studied the reaction of low-mass stars to anisotropic irradiation and its implications for the long-term evolution of compact binaries. For this we have shown that the case of anisotropic irradiation in close binaries is relevant and that spherically symmetric irradiation is probably not an adequate approximation. We have studied the reaction of low-mass stars to anisotropic irradiation by means of simple homology considerations. We have shown in the framework of this model that if the energy outflow through the surface layers of a low-mass main sequence star is blocked over a fraction $s_{\rm eff} < 1$ of its surface, it will inflate only modestly, by about a factor $\sim (1-s_{\rm eff})^{-0.1}$ (see Eq. 17) in reaching a new thermal equilibrium, and that the maximum contribution to mass transfer due to thermal relaxation is $s_{\rm eff}$ times the value one obtains for spherically symmetric irradiation (i.e. $s_{\rm eff} = 1$). The duration of the thermal relaxation phase is $0.1\tau_{\rm ce}|\ln(1-s_{\rm eff})|$ (Eqs. 22 and 23), where $\tau_{\rm ce}$ is the thermal time scale of the convective envelope. In addition, we have carried out numerical computations of the thermal relaxation process of low-mass stars involving full stellar models and using the modified Stefan-Boltzmann law (9) as an outer boundary condition. The results of these computations (shown in Figs. 2–4) fully confirm results from homology and show that the effects caused by anisotropic irradiation are not only quantitatively but also qualitatively different from those caused by spherically symmetric irradiation.

Next we have carried out a detailed stability analysis. The criterion for stability against irradiation-induced runaway mass transfer in its most general form (arbitary irradiation geometry) is given in Eqs. (41) and (45). One of the remarkable results of this stability investigation is that it is not arbitrarily large irradiation fluxes which destabilize a system most effectively.

Rather the most effective irradiating flux is $F_{\rm irr} \approx F_0$, where F_0 is the surface flux of the unperturbed star.

The reaction of the stellar surface to irradiation is best expressed in terms of a function $g(x) = -dF/dF_{\rm irr}$, where $x = F_{\rm irr}/F_0$ is the normalized flux. General considerations show that $\mathrm{Max}(xg(x)) < 1$. For determining $g(x)$ we used a simple, analytic one-zone model for the superadiabatic convection zone. The results of this simple model (Eq. 69) are found to be in good qualitative and satisfactory quantitative agreement with results of computations involving full stellar models (see Fig. 8).

Application of our stability analysis to CVs and LMXBs yields the following results:

CVs which evolve according to the standard evolutionary paradigm, i.e. the model of disrupted magnetic braking, are stable against irradiation-induced runaway mass transfer if the mass of the (ZAMS) donor is $M_{\rm s} \lesssim 0.7{\rm M}_\odot$. This holds unless substantial consequential angular momentum losses greatly destabilize the systems. Systems in which the mass of the (ZAMS) secondary is $M_{\rm s} \gtrsim 0.7{\rm M}_\odot$ can be unstable but need not be so, depending on the efficiency of irradiation η (defined in Eq. (24)). Substantial consequential angular momentum losses can however destabilize CVs over essentially the whole range of periods of interest.

CVs with a Pop. II or an evolved secondary are inherently less stable than CVs with a Pop. I ZAMS secondary. The latter are those stars which, for a given mass, have the highest thermal inertia, making the corresponding CVs the most stable ones.

If mass transfer is unstable, we found that it must evolve through a limit cycle in which phases of irradiation-induced mass transfer alternate with phases of small (or no) mass transfer. At the peak of a cycle mass transfer proceeds on a time scale which is roughly $1/s_{\rm eff}$ times the thermal time scale of the convective envelope (see Eq. 75). With decreasing mass of the secondary the amplitude of the mass transfer cycles gets smaller and the cycles eventually disappear (after a system has become stable) because the thermal inertia of the secondary (expressed in the functions Λ and Γ defined respectively in Eqs. (41) and (45)) increases strongly (see Figs. 10 and 11). A necessary condition for the maintenance of cycles is that the thermal time scale of the convective envelope has to be much shorter ($\lesssim 0.05$) than the time scale on which mass transfer is driven.

LMXBs are very likely to be stable because a) the donor star is strongly shielded from direct irradiation over most of the hemisphere facing the X-ray source, and b) because where this is not the case, $xg(x)$, i.e. the sensitivity of the stellar surface to changes in the irradiating flux, is very small.

Acknowledgements. We acknowledge support from a Royal Society/Chinese Academy of Sciences Joint Project. ZZ acknowledges support from Chinese National Natural Science Foundation. Major parts of this work have been completed while ZZ was visiting the MPA Garching, funded by the Max-Planck-Gesellschaft. We thank Andrew King for improving the language of the manuscript and an anonymous referee for helpful comments.

Appendix A: lateral heat diffusion

Here we show that in a realistic situation the lateral temperature gradient caused by irradiating the secondary anisotropically is negligible compared to the radial temperature gradient in the subphotospheric layers and that, therefore, lateral energy transport by radiation is unimportant. We demonstrate this in the framework of the point source model. In that model we estimate the lateral gradient of $T^4_{\rm irr}$ to be

$$(\nabla T^4_{\rm irr})_\vartheta \approx \frac{T^4_{\rm irr}(\vartheta=0) - T^4_{\rm irr}(\vartheta=\vartheta_{\max})}{R_{\rm s}\vartheta_{\max}} = \frac{T^4_{\rm irr}(\vartheta=0) - T^4_0}{R_{\rm s}\vartheta_{\max}} \; . \tag{A.1}$$

On the other hand, the radial temperature stratification is given by the Eddington approximation (e.g. Tout et al. 1989)

$$T^4(\tau,\vartheta) = \frac{3}{4}\left(T^4_{\rm irr}(\vartheta) - \frac{F_{\rm irr}(\vartheta)}{\sigma}\right)\left(\tau+\frac{2}{3}\right) + \frac{F_{\rm irr}(\vartheta)}{\sigma} \; , \tag{A.2}$$

where τ is the optical depth. Therefore

$$(\nabla T^4)_r = \frac{dT^4(\tau,\vartheta)}{dr} = \frac{3}{4}\left(T^4_{\rm irr}(\vartheta) - \frac{F_{\rm irr}(\vartheta)}{\sigma}\right)\frac{d\tau}{dr} \tag{A.3}$$

and

$$\mathrm{Min}|(\nabla T^4)_r| = \frac{3}{4}\left(T^4_{\rm irr}(\vartheta=0) - \frac{F_{\rm irr}(\vartheta=0)}{\sigma}\right)\frac{d\tau}{dr} \; . \tag{A.4}$$

From the definition of the optical depth we have

$$\frac{d\tau}{dr} = -\kappa\varrho \; . \tag{A.5}$$

Inserting (A.5) into (A.4) yields the minimum radial temperature gradient in the presence of irradiation:

$$\mathrm{Min}|(\nabla T^4)_r| = \frac{3}{4}\left(T^4_{\rm irr}(\vartheta=0) - \frac{F_{\rm irr}(\vartheta=0)}{\sigma}\right)\kappa\varrho \; . \tag{A.6}$$

Combining now (A.1) and (A.6) we obtain

$$\mathrm{Max}|\frac{(\nabla T^4)_\vartheta}{(\nabla T^4)_r}| \approx \frac{4}{3\vartheta_{\max}}\,\frac{T^4_{\rm irr}(\vartheta=0) - T^4_0}{T^4_{\rm irr}(\vartheta=0) - F_{\rm irr}(\vartheta=0)/\sigma}\,\frac{1}{\kappa\varrho R_{\rm s}} \; . \tag{A.7}$$

Now, because $4/3\vartheta_{\max} \approx 1$ and in the subphotospheric layers $\kappa\varrho H_{\rm P} \approx 1$, we have

$$\mathrm{Max}|\frac{(\nabla T^4)_\vartheta}{(\nabla T^4)_r}| \approx \frac{H_{\rm P}}{R_{\rm s}}\,\frac{T^4_{\rm irr}(\vartheta=0) - T^4_0}{T^4_{\rm irr}(\vartheta=0) - \frac{F_{\rm irr}(\vartheta=0)}{\sigma}} = \frac{H_{\rm P}}{R_{\rm s}}\,\frac{G(x(\vartheta=0)) + x(\vartheta=0) - 1}{G(x(\vartheta=0))} . \tag{A.8}$$

Because in the stars in question $H_{\rm P}/R_{\rm s} \approx 10^{-4}$ is so small, the lateral temperature gradient is always much smaller than the radial one unless $x(\vartheta=0) \gg 1$ and thus $G(x(\vartheta=0)) \ll 1$. However, in the range of interest of x and $G(x)$, i.e. where $xg(x)$ is near its maximum and $x \approx 1$ to a few, (A.8) yields that the lateral temperature gradient is of order $(\nabla T)_\vartheta \approx H_{\rm P}/R_{\rm s}(\nabla T)_r \ll (\nabla T)_r$.

References

Acker A., Stenholm B., 1990, A&A 233, L21
Baraffe I., Kolb U., 2000, MNRAS in press, astro-ph/0004310
Bell S.A., Pollacco D.L., Hilditch R.W., 1994, MNRAS 270, 449
Bond H.E., Grauer A.D., 1987, In: Phillip A.G.D., Hayer D.S., Liebert J. (eds.) Second Conference on Faint Blue Stars. IAU Coll. No. 95, L. Davies Press, Schenectady, p. 221
Catalán M.S., Davey S.C., Sarna M.J., Smith R.C., Wood J.H., 1994, MNRAS 269, 879
Chen A., O'Donoghue D., Stobie R.S., et al., 1995, MNRAS 275, 100
D'Antona F., Ergma E., 1993, A&A 269, 219
Ferguson D.H., Liebert J., Haas S., Napiwotzki R., James T.A., 1999, ApJ 518, 866
Frank J., King A.R., Lasota J.-P., 1992, ApJ 385, L45
Fujimoto M.Y., 1982, ApJ 257, 752
Gontikakis C., Hameury J.-M., 1993, A&A 217, 118
Grauer A.D., 1985, In: Lamb D.Q., Patterson J. (eds.) Cataclysmic Variables and Low-Mass X-ray Binaries. D. Reidel, Dordrecht, p. 29
Grauer A.D., Bond H.E., 1983, ApJ 271, 259
Grauer A.D., Bond H.E., Ciardullo R., Fleming T.A., 1987, BAAS 19, 643
Greiner J., 1996, In: Greiner J. (ed.) Supersoft X-ray Sources. LNP 472, Springer, Berlin, p. 299
Haefner R., 1989, A&A 213, L15
Hameury J.-M., 1991, A&A 243, 419
Hameury J.-M., Ritter H., 1997, A&AS 123, 273
Hameury J.-M., King A.R., Lasota J.-P., Raison, F., 1993, A&A 277, 81
Harpaz A., Rappaport S.A., 1991, ApJ 383, 739
Hilditch R.W., Harries T.J., Hill G., 1996, MNRAS 279, 1380
Kilkenny D., O'Donoghue D., Koen C., Lynas-Gray A.E., van Wyk F., 1998, MNRAS 296, 329
Kilkenny D., Penfold J.E., Hilditch R.W., 1979, MNRAS 187, 1
King A.R., 1988, QJRAS 29, 1
King A.R., 1995, In: Bianchini A., Della Valle M., Orio M. (eds.) Cataclysmic Variables. Kluwer Academic Publ., Dordrecht, p. 523
King A.R., Kolb U., 1995, ApJ 439, 330
King A.R., van Teeseling A., 1998, A&A 338, 965
King A.R., Frank J., Kolb U., Ritter H., 1995, ApJ 444, L37
King A.R., Kolb U., Burderi L., 1996a, ApJ 464, L127
King A.R., Frank J., Kolb U., Ritter H., 1996b, ApJ 467, 761
King A.R., Frank J., Kolb U., Ritter H., 1997, ApJ 482, 919
Kippenhahn R., Weigert A., 1994, Stellar Structure and Evolution. Springer Verlag, Berlin
Kohoutek L., Schnur G.F.O., 1982, MNRAS 201, 21
Kolb U., Baraffe I., 2000, New Astron. Rev. 44, 99
Kolb U., Ritter H., 1990, A&A 236, 385
Kolb U., Ritter H., 1992, A&A 254, 213
Kraft R.P., Mathews J., Greenstein J.L., 1962, ApJ 136, 312
Kudritzki R.P., Simon K.P., Lynas-Gray A.E., Kilkenny D., Hill P.W., 1982, A&A 106, 254
Kulkarni S.R., Narayan R., 1988, ApJ 335, 755
Landolt A.U., Drilling J.S., 1986, AJ 91, 1372
Mazzitelli I., 1989, ApJ 340, 249
McCormick P., Frank J., 1998, ApJ 500, 923
Mestel L., Spruit H.C., 1987, MNRAS 226, 57
Nauenberg M., 1972, ApJ 175, 417
Podsiadlowski Ph., 1991, Nat 250, 136
Pollacco D.L., Bell S.A., 1993, MNRAS 262, 377
Pollacco D.L., Bell S.A., 1994a, MNRAS 267, 452
Pollacco D.L., Bell S.A., 1994b, MNRAS 270, 449
Ritter H., 1984, A&A 145, 227
Ritter H., 1988, A&A 202, 93
Ritter H., 1994, In: D'Antona F., Caloi V., Maceroni C., Giovanelli F. (eds.) Evolutionary Links in the Zoo of Interacting Binaries. Mem. Soc. Astron. Ital. 65, p. 173
Ritter H., 1996, In: Wijers R.A.M.J., Davies M.B., Tout C.A. (eds.) Evolutionary Processes in Binary Stars. NATO ASI Series C, Vol.477, Kluwer Academic Publishers, Dordrecht, p. 223
Ritter H., 1999, MNRAS 309, 360
Ritter H., 2000, New Astron. Rev. 44, 105
Ritter H., Zhang Z., Kolb U., 1995, In: Bianchini A., Della Valle M., Orio M. (eds.) Cataclysmic Variables. Kluwer Academic Publishers, Dordrecht, p. 479
Ritter H., Zhang Z., Kolb U., 1996a, In: van Paradijs J., et al. (eds.) Compact Stars in Binaries. IAU Symp. No. 165, Kluwer Academic Publishers, Dordrecht, p. 65
Ritter H., Zhang Z., Hameury J.-M., 1996b, In: Evans A., Wood J.H. (eds.) Cataclysmic Variables and Related Objects. IAU Coll. No. 158, Kluwer Academic Publishers, Dordrecht, p. 449
Schmidt G.D., Smith P.S., Harvey D.A., Grauer A.D., 1994, AJ 110, 398
Shahbaz T., Groot P., Phillips S.N., Charles P.A., van Paradijs J., 2000, MNRAS submitted, astro-ph/0001227
Spruit H.C., Ritter H., 1983, A&A 124, 267
Stehle R., Ritter H., Kolb U., 1996, MNRAS 279, 581
Stehle R., Kolb U., Ritter H., 1997, A&A 320, 136
Tout C.A., Eggleton P.P., Fabian A.C., Pringle J.E. 1989, MNRAS 238, 427
van Teeseling A., King A.R., 1998, A&A 338, 957
Verbunt F., Zwaan C., 1981, A&A 100, L7
Vilhu O., Ergma E., Fedorova A., 1994, A&A 291, 842
Wlodarczyk K., Olszewski P., 1994, A&A 44, 407
Wood J.H., Robinson E.L., Zhang E.-H., 1995, MNRAS 277, 87
Wood J.H., Saffer R., 1999, MNRAS 305, 820